COMPARISON OF DOSE DISTRIBUTION FOR DIFFERENT TECHNIQUES OF BREAST IRRADIATION TREATMENT

LIBRARY AND INFORMATION CENTER
MAHIDOL UNIVERSITY

PACHUEN POTUP

A THESIS SUBMITTED IN PARTIAL FULFILLMENT

OF THE REQUIREMENT FOR

THE DEGREE OF MASTER OF SCIENCE

(MEDICAL PHYSICS)

FACULTY OF GRADUATE STUDIES

MAHIDOL UNIVERSITY

1998

ISBN 974-661-534-3

COPYRIGHT OF MAHIDOL UNIVERSITY

TH
P116C
1998

With compliments
of
มหาวิทยาลัยมหิดล

Copyright by Mahidol University

Thesis

entitled

COMPARISON OF DOSE DISTRIBUTION FOR DIFFERENT TECHNIQUES OF BREAST IRRADIATION TREATMENT

Pachuen Potup

Pachuen Potup
Candidate

Sivalee Suriyapee

Sivalee Suriyapee, M.Eng.
Major advisor

Ratana Pirabul

Ratana Pirabul, M.Sc.
Co-advisor

Nopadol Asavametha

Nopadol Asavametha, M.D.
Co-advisor

Adulya Viriyavejakul

Adulya Viriyavejakul
M.D., LL.B., F.R.C.P.
Dean
Faculty of Graduate Studies

Ratana Pirabul

Ratana Pirabul, M.Sc.
Chairman
Master of Science Programme
In Medical Physics
Fuculty of Medicine,
Ramathibodi Hospital

Copyright by Mahidol University

Thesis

entitled

COMPARISON OF DOSE DISTRIBUTION FOR DIFFERENT TECHNIQUES OF BREAST IRRADIATION TREATMENT

was submitted to the Faculty of Graduate Studies, Mahidol University
for the degree of Master of Science (Medical Physics)

On
September 22, 1998

Pachuen Potup
Pachuen Potup
Candidate

Sivalee Suriyapee
Sivalee Suriyapee, M.Eng.
Chairman

Nopadol Asavametha
Nopadol Asavametha, M.D.
Member

Paranee Sahachjesdakul
Paranee Sahachjesdakul, M.Sc.
Member

Ratana Pirabul
Ratana Pirabul, M.Sc.
Member

Adulya Viriyavejakul
Adulya Viriyavejakul
M.D., LL.B., F.R.C.P.
Dean
Faculty of Graduate Studies

B. Pongpanich
Boonchob Pongpanich,
D.C.H, F.A.C.C.
Dip. Amer. Board of Ped.
Dean
Fuculty of Medicine,
Ramathibodi Hospital

Copyright by Mahidol University

ACKNOWLEDGEMENT

I would like to express my sincere gratitude and deep appreciation to Assoc. Prof. Sivalee Suriyapee and Assist. Prof. Nopadol Asavametha at the Department of Radiology, Faculty of Medicine, Chulalongkorn Hospital for the suggestion of this thesis and for helpful advice, guidance throughout this work and reviewing with correcting the manuscript.

Special gratitude is expressed to Assist. Prof. Praphatson Rajatatiti, M.D. the Head of Radiation Oncology, Chulalongkorn Hospital for her supporting on the use of equipment for these experiments. Thanks also to Mr. Vrajin Bunkong and Ms. Wannapa Maytapirak for their technical ability of the technique in patient set-up. Also my sincere thanks go to all of the staff of this hospital for their friendship and good cooperation.

I wish to express to Prof. Dr. Puangtong Kraipibul, Head of the Department of Radiology, Ramathibodi Hospital, for her support and use of the equipment.

I also express my appreciation to the committee, Assist. Prof. Ratana Pirabul and Archan Paranee Sahachjesdakul.

I would like to thank Ms. Chotika Jumpangern for her great assistance in technical of irradiation and wonderful friendships.

I am also thankful to the school of Medical Physics, Mahidol University, for supplying me academic knowledge on Medical Physics.

Finally, I would like to mention immeasurable contribution and encouragement of my father, mother, brothers and my family for their support to my spirits during the entire course of study.

Pachuen Potup

Copyright by Mahidol University

3936127 RAMP/M : MAJOR: MEDICAL PHYSICS; M.Sc. (MEDICAL PHYSICS)
KEY WORD : BREAST IRRADIATION / TANGENTIAL / HALF-BEAM BLOCK / SURFACE DOSE

PACHUEN POTUP : COMPARISON OF DOSE DISTRIBUTION FOR DIFFERENT TECHNIQUES OF BREAST IRRADIATION TREATMENT. THESIS ADVISOR : SIVALEE SURIYAPEE M.Eng., NOPADOL ASAVAMETHA M.D., 101 p. ISBN 974-661-534-3

The study of dose distribution for different techniques of breast and chest wall irradiation treatment was under taken to determine the best method for improving homogeneity of dose in the treated breast and reducing the dose delivered to tissue outside the treatment volume. The dose in lung tissue and surface dose to target and to contralateral breast were considered. This study used a Clinac 1800 linear accelerator set to produce 6 MV x-rays, a rando phantom tissue-equivalent model and two patients who were undergoing conservative breast treatment. Dose measurements were made by using thermoluminescence dosimeters (TLD-100 chips). The irradiation treatment was conducted using opposing tangential field technique with source to skin distance (SSD) of 100 cm. Asymmetric half beam created using asymmetric collimators and symmetric beam created using symmetric collimators were both used in this study. All techniques were tested without the wedge beam accessory, and with both 15° and 30° wedges used as compensators.

For all techniques, the absorbed dose at reference points in the rando phantom breast model are very close to the prescribed dose of 200 cGy. The upper transverse plane shows higher dose and the lower transverse plane shows lower dose than the central plane. The absorbed dose in the lower plane of asymmetric beams is lower than that of symmetric beams. The use of asymmetric beams results in somewhat poorer homogeneity of radiation dose to the target breast than the use of symmetric beams. Wedge filters are not ideal compensators use in the irradiation treatment of breasts. The average doses to chest wall and lung in all techniques are increased when larger degree of wedge angle is used and doses are decreased significantly when asymmetric beams are used. Finally, the surface doses on target breast phantom and patients are decreased significantly when larger degree of wedge is used, but the surface doses at the contralateral breast are higher when larger degree of wedge angle is used, but the surface doses to the contralateral breast are higher when larger degree of wedge angle is used. The behavior of surface doses in both the target and contralateral breasts of the patients irradiated by symmetric and asymmetric beams are different from the behavior of the doses to the phantom due to variations of individual patients size and shape. Due to the variations in patients breast shape and size, as well as the small number of patients, it is difficult to compose the patient's results to the rando phantom results in this study.

Copyright by Mahidol University

3936127 RAMP/M : สาขาวิชา : ฟิสิกส์การแพทย์ ; วท.ม. (ฟิสิกส์การแพทย์)

พาชื่น โพทัพ : การเปรียบเทียบการกระจายปริมาณรังสีของการรักษามะเร็งเต้านม เทคนิคแบบต่างๆ (Comparison of dose distribution for different techniques of breast irradiation treatment) คณะกรรมการควบคุมวิทยานิพนธ์ : ศิวลี สุริยาปี M,Eng., นพดล อัศวเมธา M.D.,
101 หน้า ISBN 974-661-534-3

การเปรียบเทียบการกระจายของปริมาณรังสีในเทคนิคต่างๆ สำหรับการฉายรังสีที่เต้านม และผนังทรวงอก รวมถึงปริมาณรังสีในส่วนของเนื้อเยื่อปอดและส่วนของเต้านมด้านที่ฉายรังสี และด้านตรงข้ามได้รับ โดยใช้เครื่องเร่งอนุภาค Varian Clinac 1800 ที่พลังงาน 6 MV และใช้ rando phantom และผู้ป่วย สำหรับเครื่องวัดรังสีที่ใช้คือ TLD-100 ชนิด chip เทคนิคของการฉายรังสีที่ศึกษาในครั้งนี้คือ การฉายรังสีแบบ two opposing tangential fields ที่ระยะจากแหล่งกำเนิดถึงผิวเท่ากับ 100 เซนติเมตร แบ่งออกเป็น symmetric และ asymmetric โดยใช้ asymmetric collimators ซึ่งในแต่ละเทคนิคจะประกอบด้วย beams ที่มีและไม่มี wedge filter

จากการทดลอง พบว่าในทุกเทคนิค ค่าปริมาณรังสีที่จุดอ้างอิงในระนาบตัดขวางของแนวแกนกลางลำรังสี ในหุ่นจำลองเต้านม จะมีค่าเข้าใกล้ค่าปริมาณรังสีที่กำหนด คือ 200 cGy ที่จุดในระนาบเหนือแนวแกนกลาง 2.5 ซม ค่าปริมาณรังสีจะสูง และที่ระนาบต่ำกว่าแนวแกนกลาง 2.5 ซม ค่าปริมาณรังสีจะต่ำ ค่าปริมาณรังสีในระนาบล่างของ asymmetric beams จะต่ำกว่าใน symmetric beams ซึ่งใน asymmetric beams ไม่ได้มีส่วนช่วยให้เกิดความสม่ำเสมอของค่าปริมาณรังสีในเต้านมด้านที่ฉาย เมื่อเทียบกับ symmetric beams และ wedge filter ไม่ได้ชดเชยเนื้อเยื่อที่ขาดไปในแนวโค้งของเต้านมอย่างสมบูรณ์ในทุกระนาบ สำหรับค่าปริมาณรังสีเฉลี่ยของผนังทรวงอกและปอดในทุกเทคนิค พบว่า จะมีการเพิ่มขึ้นเมื่อมุมของ wedge เพิ่ม และมีค่าลดลงเมื่อใช้ asymmetric beams ในท้ายสุด ปริมาณรังสีที่ผิวเต้านมบนหุ่นจำลอง และในผู้ป่วยจะมีค่าลดลง เมื่อใช้ wedge ที่มีมุมมากขึ้น แต่ปริมาณรังสีที่ผิวบนเต้านมด้านตรงข้ามจะมีค่าเพิ่มขึ้น เมื่อมุมของ wedge เพิ่มขึ้นด้วย การแสดงออกของปริมาณรังสีที่ผิว ทั้งในเต้านมด้านที่ฉายและด้านตรงข้ามในผู้ป่วย จะแตกต่างไปจากหุ่นจำลอง ความแตกต่างนี้อาจเกิดจาก ขนาดและรูปร่างของผู้ป่วยที่ต่างจากหุ่น และ จากการวัดในผู้ป่วยที่มีจำนวนน้อยเกินไป

Copyright by Mahidol University

CONTENTS

	Page
ACKNOWLEDGEMENT	iii
ABSTRACT	iv
LIST OF TABLES	vii
LIST OF FIGURES	x
LIST OF ABBREVIATIONS	xiv
CHAPTER	
I INTRODUCTION	1
II THEORY	4
2.1 Treatment planning of breast	4
2.2 Basic dosimetry of asymmetric x-ray collimators	10
2.3 Thermoluminescence dosimetry	16
III OBJECTIVES	22
IV MATERIALS AND METHODS	23
4.1 Materials	23
4.2 Methods	28
V RESULTS	39
VI DISCUSSION AND CONCLUSION	78
REFERENCES	82
BIOGRAPHY	85

Copyright by Mahidol University

LIST OF TABLES

		Page
Table 1	The absorbed dose measurement at various points in the breast phantom in the mid coronal plane in symmetric beams.	43
Table 2	The absorbed dose measurement at various points in the breast phantom in the mid coronal plane in asymmetric beams.	43
Table 3	The comparison of dose distribution of target breast from different techniques (the percentage relative doses).	45
Table 4	The absorbed dose measurement at various points in the17th slab of the chest rando phantom which is the central plane in symmetric beams.	48
Table 5	The absorbed dose measurement at various points in the17th slab of the chest rando phantom which is the central plane in asymmetric beams.	48
Table 6	The absorbed dose measurement at various points in the15th slab of the chest rando phantom which is 5 cm upper off axis from the central plane in symmetric beams.	52
Table 7	The absorbed dose measurement at various points in the15th slab of the chest rando phantom which is 5 cm upper off axis from the central plane in asymmetric beams.	52
Table 8	The absorbed dose measurement at various points in the19th slab of the chest rando phantom which is 5 cm lower off axis from the central plane in symmetric beams.	56

Copyright by Mahidol University

LIST OF TABLE (Continued)

		Page
Table 9	The absorbed dose measurement at various points in the19th slab of the chest rando phantom which is 5 cm lower off axis from the central plane in asymmetric beams.	56
Table 10	The comparison of dose distribution in the chest wall from different techniques (the percentage relative doses) at the center, 5 cm upper and 5 cm lower to the central plane, respectively.	60
Table 11	The comparison of dose distribution in the lung tissue from different techniques (the percentage relative doses) at the center, 5 cm upper and 5 cm lower to the central plane, respectively.	61
Table 12	The variation of the percentage relative surface dose on the rando phantom with different wedge angles in symmetric beams techniques.	64
Table 13	The variation of the percentage relative surface dose on the rando phantom with different wedge angles in asymmetric beams techniques.	64
Table 14	The variation of the percentage relative surface dose on the rando phantom with different wedge angles in symmetric beams techniques at the contralateral breast.	70
Table 15	The variation of the percentage relative surface dose on the rando phantom with different wedge angles in asymmetric beams techniques at the contralateral breast.	70
Table 16	The variation of the percentage relative surface dose on the patients with different wedge angles in symmetric beams techniques.	73

Copyright by Mahidol University

LIST OF TABLE (Continued)

		Page
Table 17	The variation of the percentage relative surface dose on the patients with different wedge angles in asymmetric beams techniques.	73
Table 18	The variation of the percentage relative surface dose on the patients with different wedge angles in symmetric beams techniques at the contralateral breast.	76
Table 19	The variation of the percentage relative surface dose on the patients with different wedge angles in asymmetric beams techniques at the contralateral breast.	76

Copyright by Mahidol University

LIST OF FIGURES

	Page
Fig. 1 Isodose distribution resulting from parallel opposed tangential fields to the breast of a large breast patient with and without wedges.	5
Fig. 2 Isodose distribution in three level of 4 MV photons with SSD technique and 30° wedge were used.	6
Fig. 3 An anterior 4 MV photon beam yields a high dose in underlying normal tissue and combining 4 MV photon and 12 MeV electron.	7
Fig. 4 Breast contour (central contour of phantom).	8
Fig. 5 Asymmetric and symmetric beams measured isodose curve for 6 MV x-rays passing through 5,10,15,20,25 and 30 cm depth in water.	11
Fig. 6 Geometry of field blocking by an independent jaw.	13
Fig. 7 Isodose distribution for a 45° wedge filter for symmetric and half-collimated fields.	14
Fig. 8 The Clinac 1800 linear accelerator.	25
Fig. 9 The Alderson Rando phantom.	26
Fig. 10 The Harshaw Model 5500 automatic TL reader.	27
Fig. 11 The absorbed dose measurement at various points in the 15^{th} slab of the rando phantom in symmetric and asymmetric beams	29
Fig. 12 The absorbed dose measurement at various points in the 16^{th} slab of the rando phantom in symmetric and asymmetric beams.	30

Copyright by Mahidol University

LIST OF FIGURES (Continued)

Page

Fig. 13 The absorbed dose measurement at various points in the 17th slab of the rando phantom in symmetric and asymmetric beams. 31

Fig. 14 The absorbed dose measurement at various point in the 18th slab of the rando phantom in symmetric and asymmetric beams. 32

Fig. 15 The absorbed dose measurement at various points in the 19th slab of the rando phantom in symmetric and asymmetric beams. 33

Fig. 16 The surface dose measurement at various points on the target and contralateral breast of the rando phantom in symmetric and asymmetric beams. 34

Fig. 17 Symmetric beams technique of tangential fields. 36

Fig. 18 Asymmetric beams technique of tangential fields. 37

Fig. 19 The TLD positions on surface of target and contralateral breast on the patients. 38

Fig. 20 The various points in the breast phantom in the transverse plane in the 16th 17th and 18th slabs of the rando phantom. 41

Fig. 21 The region of the mid coronal plane and the various points in the breast phantom. 42

Fig. 22 Comparison of dose at various points in the breast phantom in symmetric and asymmetric beams. 44

Fig. 23 The absorbed dose measurement at various points in the 17th slab of the rando phantom which is the central plane by open beam technique in symmetric and asymmetric beams. 49

Copyright by Mahidol University

LIST OF FIGURES (Continued)

Page

Fig. 24 The absorbed dose measurement at various points in the 17th slab of the rando phantom which is the central plane by 15°wedged beam technique in symmetric and asymmetric beams. 50

Fig. 25 The absorbed dose measurement at various points in the 17th slab of the rando phantom which is the central plane by 30° wedged beam technique in symmetric and asymmetric beams. 51

Fig. 26 The absorbed dose measurement at various points in the 15th slab of the rando phantom which is 5 cm upper off axis from the central plane by open beam technique in symmetric and asymmetric beams. 53

Fig. 27 The absorbed dose measurement at various points in the 15th slab of the rando phantom which is 5 cm upper off axis from the central plane by 15° wedged beam technique in symmetric and asymmetric beams. 54

Fig. 28 The absorbed dose measurement at various points in the 15th slab of the rando phantom which is 5 cm upper off axis from the central plane by 30°wedged beam technique in symmetric and asymmetric beams. 55

Fig. 29 The absorbed dose measurement at various points in the 19th slab of the rando phantom which is 5 cm lower off axis from the central plane by open beam technique in symmetric and asymmetric beams. 57

Fig. 30 The absorbed dose measurement at various points in the 19th slab of the rando phantom which is 5 cm lower off axis from the central plane by 15° wedged beam technique in symmetric and asymmetric beams 58

Copyright by Mahidol University

.LIST OF FIGURES (Continued)

Page

Fig. 31 The absorbed dose measurement at various points in the 19th slab of the rando phantom which is 5 cm lower off axis from the central plane by 30° wedged beam technique in symmetric and asymmetric beams 59

Fig. 32 The percentage relative surface dose which is in the central plane by open beam technique in symmetric and asymmetric beams. 65

Fig. 33 The percentage relative surface dose which is in the central plane by 15° wedged beam technique in symmetric and asymmetric beams. 66

Fig. 34 The percentage relative surface dose which is in the central plane by 30° wedged beam technique in symmetric and asymmetric beams. 67

Fig. 35 Comparison of the percentage relative surface dose to the breast phantom of symmetric and asymmetric beams with and without wedges. 68

Fig. 36 Comparison of the percentage relative surface dose at point #1 of the contralateral breast in different techniques. 71

Fig. 37 Comparison of the percentage relative surface dose to the breast on the patients in symmetric and asymmetric beams with and without wedges. 74

Fig. 38 Comparison of the percentage relative surface dose at point #1 of the contralateral breast in the patients in different techniques. 77

Copyright by Mahidol University

LIST OF ABBREVIATIONS

Abbreviation	Term
Asym	Asymmetric
cGy	centi Gray
^{60}Co	Cobalt-60
°C	Degree Celsius
d_m	Depth of maximum dose
D	Absorbed dose
ECC	Element Correction Coefficient
FS	Field size
Gy	Gray
IMC	Internal mammary chain
L	The calibration absorbed dose
LiF	Lithium Fluoride
MV	Megavoltage
MeV	Megaelectron volt
Mu	Monitor unit
Mg	Magnesium
nC	nanocoulomb
nC/mR	nanocoulomb per miliroentgen
OAR	Off-axis ratio
P	Percentage depth dose

Copyright by Mahidol University

LIST OF ABBREVIATIONS (Continued)

Abbreviation	Term
PMT	Photomultiplier tube
Q	Charge integral
RCF	Reader Calibration Factor
Sym	Symmetric
Sc	Collimator scatter factor
Sp	Phantom scatter factor
TF	Tray factor
TL	Thermoluminescence
Ti	Titanium
UV	Ultraviolet
WF	Wedge factor
Zeff	Effective atomic number

Copyright by Mahidol University

CHAPTER I

INTRODUCTION

In Thai women, breast cancer is the most common malignancy. It accounts for 22.59% all female patients (1). The first major use of radiation therapy in the treatment of primary breast cancer is to reduce locoregional recurrence rates following radical mastectomy. Radiation therapy is also used to treat locally advanced and metastatic disease. More recently, radiation therapy has been used in combination with conservative surgery as an option for patients who prefer breast conserving treatment.

The target volume generally includes the breast, chest wall and regional lymph nodes. Breast and chest wall are most frequently treated via opposed tangential fields while the supraclavicular and sometimes also the axillary lymph nodes are treated with a separate anterior field. When necessary, internal mammary nodes are treated by tangential fields or an en face field of photon or electrons.

Treatment techniques for the patients of breast cancer are very complex . Due to many variations which are :

(1). The patient's size.

(2). The breast size and shape.

(3). The presence or absence of the breast.

(4). The patient's ability to elevate the arm.

Copyright by Mahidol University

A number of important and challenging technical issues have been shown to influence successful outcome of this therapy, these include:

(a). homogeneity and distribution of dose.

(b). coverage of a highly complex target.

(c). ease of set up.

Other important considerations include dose to normal tissues which are the heart, lungs and contralateral breast (2). Delivering uniform dose to the entire breast is usually difficult due to the irregular shape of the breast tissue, causing varying degree of attenuation. Wedges are used in an attempt to improve the dose uniformity within the tangential fields.

The problem concerned in treatment of tangential fields are beam divergence that the chest wall is curved and the depth of the lung below the breast tissue is small (approximately 2 cm), cause the difficulty in avoiding irradiation of the lung (3). However breast irradiation, tangential fields contribute the scatter dose to contralateral breast.The contralateral breast dose from primary breast irradiation has been implicated in the risk of second breast malignancies (2). Futhermore, breast treatment technique where the radiation dose delivered to the skin can cause severe reaction and/or bad cosmetic results.

Rossnow, et. al.(4) recently published a method by which a nondivergent edge is achieved at the tangential cephalad border by using asymmetric jaws in a linear accelerator. Their technique relied on collimator angulation to follow the chest wall for tangential portals. They have developed monoisocentric technique for the three fields treatment of early breast cancer which avoids the use of heavy block and the higher transmission that permit as compare to the collimator transmission.

Copyright by Mahidol University

The technique is inherent easy and accurate, allow for the symmetric irradiation of the breast, and for easy quality control prior to the first treatment. But there are two disadvantages to this technique. The first is that maximum field length at 100 SAD is 40 cm ; therefore the maximum half-beam length for the tangential is 20 cm The second is that wedges covering both halves of the length are not available.

Copyright by Mahidol University

CHAPTER II

THEORY

2.1 Treatment planning of breast

The treatment technique necessary for the breast and the regional nodes, without delivering excessive doses to underlying lung, are very complex and require very careful treatment planning and daily set up. The tangential fields across the chest wall or breast result in higher dose close to the skin surface or the apex of the breast in (Fig.1). Wedges or compensator may be necessary to reduce this "hot spot". Before applying wedges one should evaluate the dose distribution in other levels as well. In the technique described, where customized blocks are used to shape the tangential fields, the block intercept almost half of the beam and the center of wedge. The field is therefore wedged only by the thick part of the wedge at the central axis plane while at the cephalad margin the actual field is wider. Here, most of the treatment volume lies within the part of the beam which passes through the thin part of the wedge, causing the tissue dose to be somewhat higher (Fig. 2). Hot spots created in this manner are usually more pronounced in large patients,while the "hot spot" at the apex of the breast are more pronounced in patients with large breasts when no wedges are used (5).

Copyright by Mahidol University

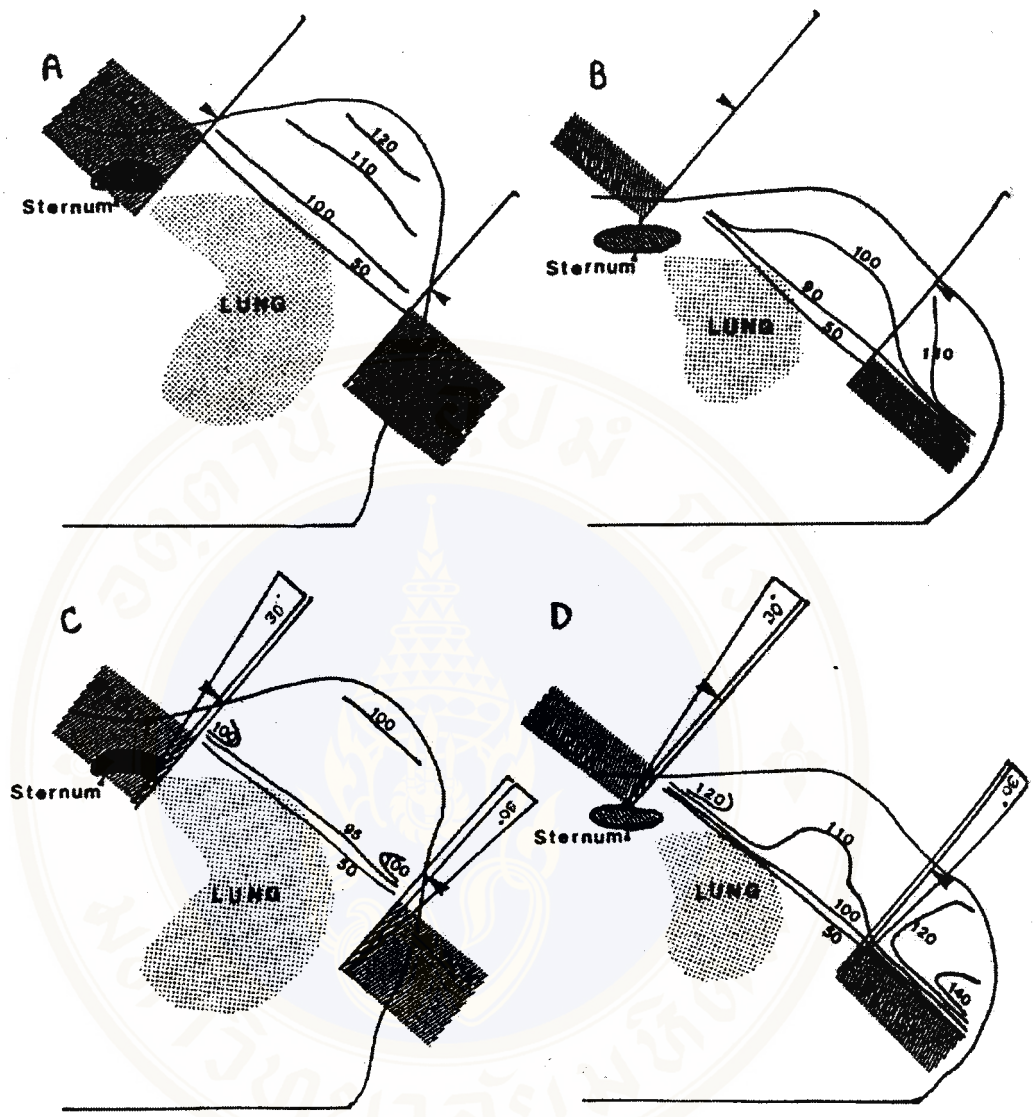

Fig. 1 (A).Isodose distribution resulting from parallel opposed unwedged tangential fields to the breast of a large breast patient.The dose range is from 100% at the deep margin of the breast to 120% at the apex. (B). Isodose distribution from the same patient without wedges but in the cephalad region.The maximum dose is in the lateral posterior aspect of the chest wall. The dose deep in the chest wall is lower than in the central axis plane and is caused by the greater separation of the fields in this level. (C).Isodose distribution with 30° wedged added. The dose uniformity is increased noticeably.(D). Wedges used in the same field result in considerably higher doses in the lateral posterior aspect of the chest wall. These plane are the result of 4 MV photon beams using an SSD technique (5).

Copyright by Mahidol University

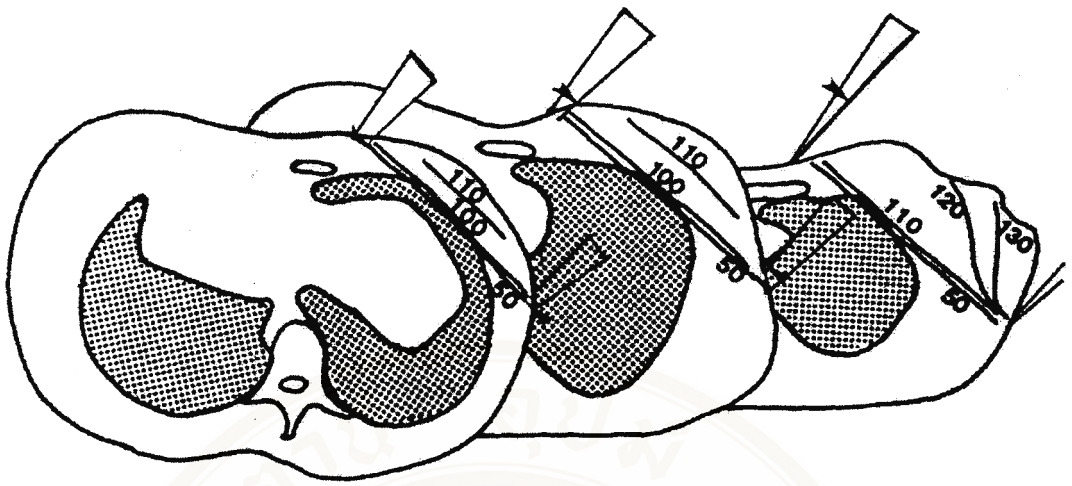

Fig. 2 Isodose distribution in three levels. The dose ranges from 100% at the chest wall in the caudad and central axis level to 130% in the lateral aspect in the cephalad level. 4 MV photons with an SSD technique and 30° wedge were used (6).

An anterior photon field, including the internal mammary nodes delivers unnecessarily high dose to deeper structures such as the esophagus and the spinal cord. Partial treatment with a 10 to 14 MeV electron beams (Fig. 3) would result in considerable sparing of the deeper normal tissue, and the photon component would provide more skin sparing than the entire treatment was delivered with an electron beam (5). However, the oblique incidence of the beam reduces the skin sparing effect of high energy photons (7).

Copyright by Mahidol University

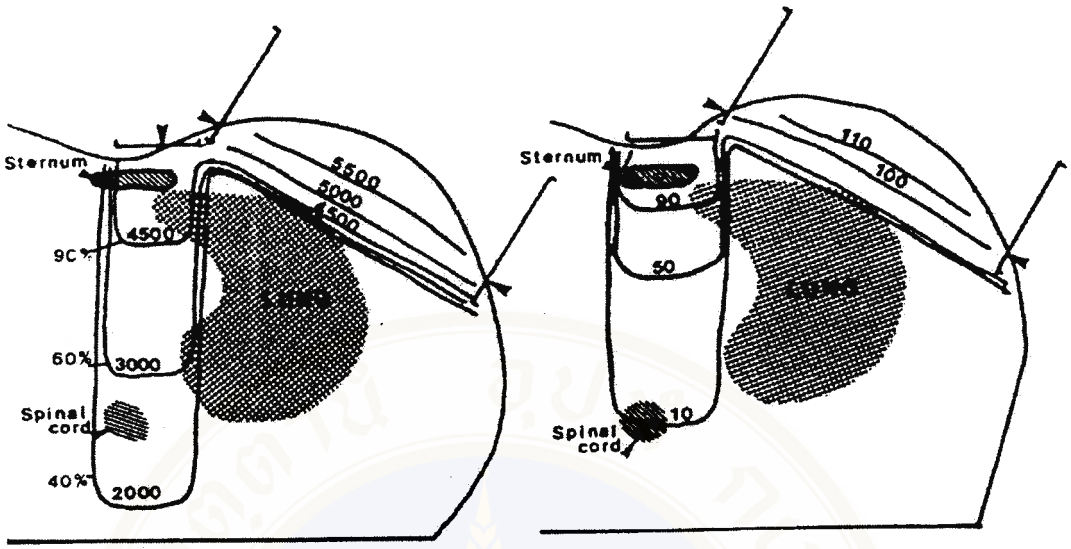

Fig. 3 An anterior 4 MV photon beam yields a high dose in underlying normal tissue (left). Combining 4 MV photon and 12 MeV Electrons reduce the dose to underlying tissue (right)(7).

2.1.1 Techniques of irradiation

(a). Simulation and localization

(1). The patient is in supine position on the simulation couch.

(2). The patient positioned appropriately , the medial and lateral tangential field borders, as well as the superior and inferior borders are marked on the patient.

(3). Using the fluoroscopic view and adjusting the table position (vertical and lateral) as well as the gantry angle, the central axis of the beam is made to align exactly with the medial and lateral markers.

(4). The extent of lung in the field is noted approximately 2-3 cm of lung to provide an adequate field margin for chest wall irradiation.

(5). On the central contour of the patient, various landmarks such as the midsternal line, medial border, lateral border and the table top are marked on this

Copyright by Mahidol University

contour and the beam geometry is reconstructed to determine the rest of the set up parameters, (Fig. 4).

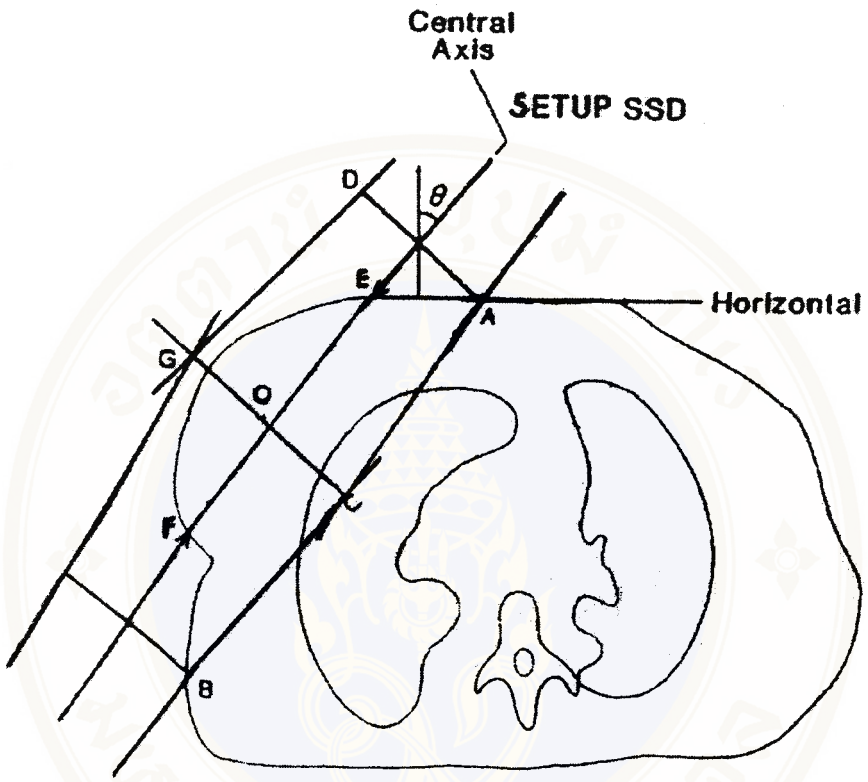

Fig. 4 Breast contour (central contour of phantom).

Point A : the medial border of tangential field.

Point B : the later border of tangential field.

Line AB : the line joining the points on the medial and lateral borders.

Line CG : designate the field width and is set to include the apex of the breast with a clearance of 1 to 2 cm.

Line EF : the central axis of beam.

Point F : the center point of lateral tangential field.

Point E : the center point of medial tangential field.

Copyright by Mahidol University

Angle θ : medial gantry angle.

From point O, line OE and OF determine the depth of medial and lateral tangential fields.

(b). Tangential fields

The two opposing tangential fields consist of medial and lateral portals tangentially to the chest wall. These portals should parallel the path of the anterior chest wall and encompass a uniform, thin volume, usually limited to 3 cm or less of underlying lung (8). The medial tangential field borders with the internal mammary segment of the anterior field and is angled such that the deep edge of the beam exits at the midaxillary line. The opposed lateral tangential field enters with its deep margin. At this point is angled such that beam edge exits at the border of anterior internal mammary field. Because of the diverging beam edges it was difficult to opposed these two beam edges (5).

Superior border : extend as far superiorly as possible (i.e. first or second intercostal space).

Inferior border : extend to a level 1 to 2 cm below the margin of breast tissue.

Medial border : at the midline if the IMC lymph nodes are not to be included and 3 cm or more across the midline if the IMC is to be included (9).

Lateral border : should be brought 1 to 2 cm lateral to the palpable edge of the breast, typically at the midaxillary line (8).

Copyright by Mahidol University

2.2 Basic dosimetry of asymmetric x-ray collimators

Conventional linear accelerator have four field-defining jaws or collimators. Usually, one set of the two opposing jaws moves concurrently to define the field width and the other set defines the field length. The resultant square or rectangular field will have the field centerline coincide with the collimator axis. However, some modern linacs have independent collimators or jaws that can be set asymmetrically (10).

An asymmetric x-ray collimator also known as an independent jaw has one or more collimating jaws that can be moved independently of the corresponding opposed jaws. This allow one to block a portion of the field from one side without affecting the opposite jaw setting.

Asymmetric collimators have found many clinical application, such as half-beam asymmetric fields. The use of two asymmetric fields adjacent to each other eliminates the problem of matching two divergent fields which produce hot and cold spots in the dose distribution , to avoid irradiating critical organs or tissues on the contralateral side by an exit beam due to beam divergence (11) and another use of a half-beam asymmetric field in tangential opposed breast technique will simplify set up and improve dose distribution.

Normally the calculation of dose and isodose distribution in a patient requires basic data which are measured with symmetric collimators (12). The dosimetric parameters of high energy photon beams which strongly depend on the design of beam collimation system are field size factors and field penumbra (13). The difference in dose between an asymmetric and a symmetric radiation field is accounted for by a correction factor that is a function of the asymmetric and symmetric field sizes, off axis distance and depth of measurement (10). Generally the change of dose

Copyright by Mahidol University

rate at a point in a phantom as a function of field size is related both to the change in collimator scatter and phantom scatter because as the collimator are open they present more surface area to the beam with concomitantly more radiation being scattered from these surfaces. Likewise, as more phantom volume is irradiated more scatter occurs in the phantom. Also the differential hardening of the beam which results in change of beam quality at off-axis points will influence the depth dose characteristics and shape of isodose curves as the field opening is moved asymmetrically from central axis (Fig.5).

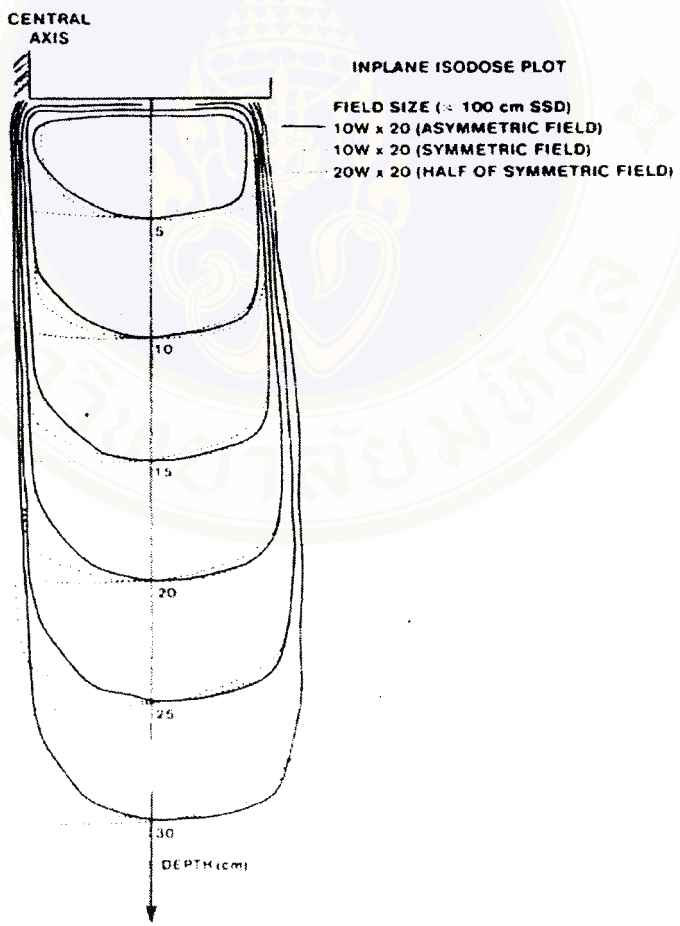

Fig. 5 Asymmetric and symmetric beams measured isodose curves for 6 MV x-rays passing through 5, 10,15,20,25 and 30 cm depth in water (13).

Copyright by Mahidol University

Dose to a point on central ray of an asymmetric field

In asymmetric fields, however, the target or the point of interest dose not lie on the beam central axis ; therefore, an off-axis dose correction will depend on the depth and the distance from the central axis of the point of interest (14).

The equations are proposed for the calculation of dose for asymmetric fields. For SSD-type of treatment verified the following :

$$D\ (d_m,x,r) = k\ Mu\ Sc(r,0)\ Sp(r,0)\ OAR_{dm}(x) \quad (1)$$

Where Mu is the number of monitor units and k is the dose per Mu, which is 1 cGy / Mu at the calibration point at depth d_m on the central axis of a symmetrical $10\times10\ cm^2$ field. Thus for calculating D_{max} dose in an asymmetric field, the output factors for symmetric fields may be used. The only additional factor required is the off-axis dose ratio $OAR_{dm}(x)$.

Similarly the dose to a point (x) at depth d on the central ray of an asymmetrically collimated field may be expressed approximately as ;

$$D\ (d,x,r) \approx k\ Mu\ Sc(r,0)\ Sp(r,0)\ P(d,0,r)\ OAR_d(x) \quad (2)$$

Where P (d,0,r) is the central axis fractional depth dose for the symmetrical field of size r×r and OAR_d (x) is the off-axis ratio derived from cross beam profile at depth d. Equation (2) shows that the depth dose at a point (d,x) on the central ray of an asymmetric field is given by the product of the dose at the same depth on the central axis of a symmetric field of the same dimensions and the off-axis ratio at that depth.

Copyright by Mahidol University

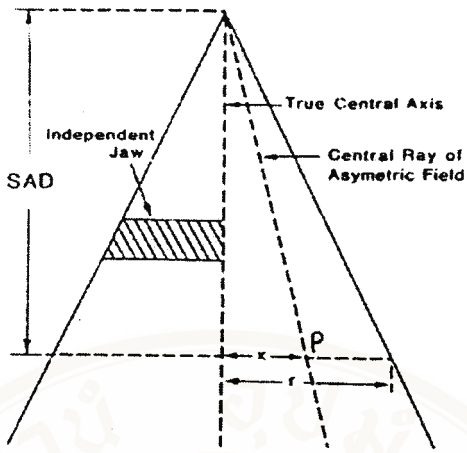

Fig. 6 Geometry of field blocking by an independent jaw : point P on the central ray of a half-beam block field and distance x from the beam central axis (12).

2.2.1 Dosimetry of wedged fields with asymmetric collimation

The shaping of wedged fields with asymmetric collimators needs to be considered when calculating isodose distribution and monitor unit settings. In the case of a wedged field additional complexity arises with regard to the use of a wedge transmission factor since the point of target dose specification may be located off-axis. If the point of calculation is moved in the wedged direction, additional correction are needed for change in wedge attenuation and scatter (15). Wedge transmission factor, WF was determined as the ratio of the dose measured with wedged field to the corresponding open field on central axis at the depth of dose maximum. The characteristics of wedge factor dependence on depth and field size for various beam energies. However, the degree of dependence at various depths and field sizes varies with wedge angle, beam energy and collimator design (16).

Copyright by Mahidol University

Wedged isodose curves for 20×20 cm^2 for symmetric and half-collimated fields for a 45° nominal wedge angle are shown in (Fig. 7) isodose values on the reference line in a half-collimated beam are similar to those on the central ray of a symmetric field for 30°, 45° and 60° wedges. Whereas, for a 15° wedge the slope of isodose lines for half-collimated settings are almost the same as that of symmetric setting (17).

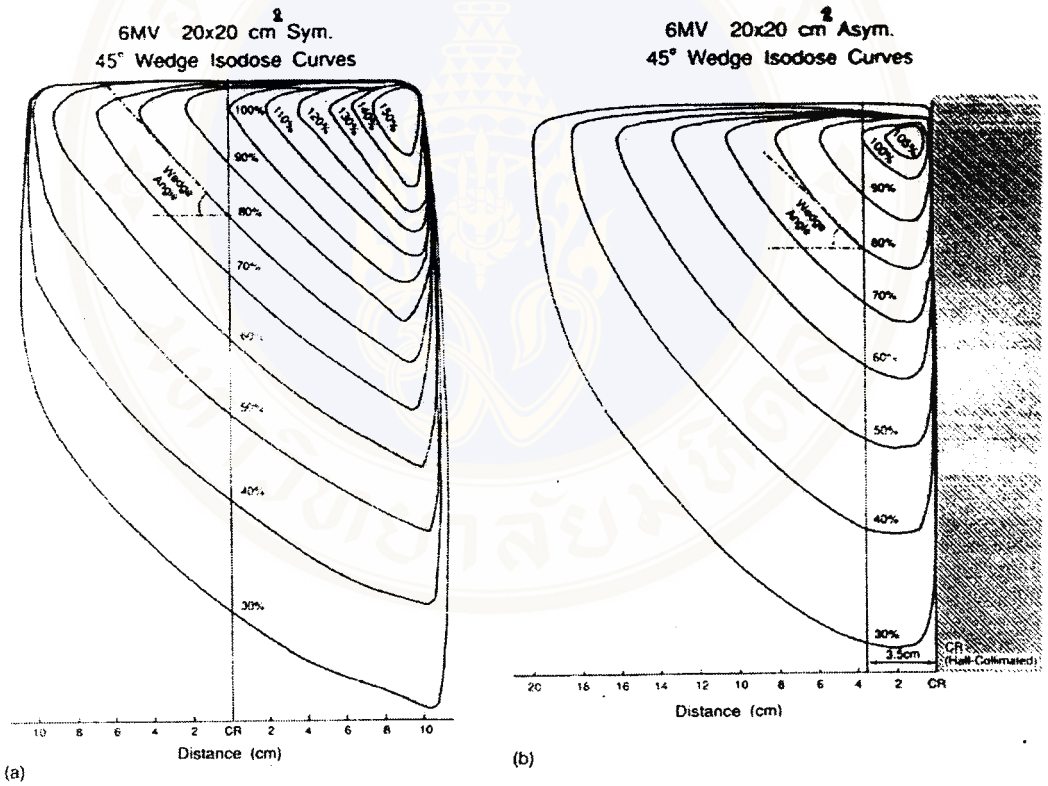

Fig. 7 Isodose distribution for a 45° wedge filter for (a). symmetric and (b). half-collimated fields (17).

Copyright by Mahidol University

Asymmetric collimators of a wedged field gives rise to changes in the scatter dose which are similar to those produced by symmetrically collimated fields. Relative changes in photon scatter due to asymmetric field changes are approximately the same for wedged beams as for unwedged beams except for large wedge angles (e.g. 60°) with extensive field changes in the wedged direction. The effect of asymmetric collimators on wedge angle is minimal (15).

In the case of wedged beam, the equation is proposed for the monitor unit calculation for SSD-type of treatment verified the following :

$$Mu = \frac{D(d,x,r)}{k\,P(d,0,r)\,Sc(r,0)\,Sp(r,0)\,OAR_{d,w}(x)\,WF\,TF} \qquad (3)$$

where $OAR_{d,w}(x)$ is the off-axis ratio at point P for a wedged beam and WF is the wedge factor determined at central axis. The factor $OAR_{d,w}(x)$ can be obtained from the symmetric wedged beam profiles or isodose curves. The wedge off-axis ratio is used to correct for changing in wedge attenuation when the point of calculation is moved in the wedged direction (15).

Copyright by Mahidol University

2.3 Thermoluminescence Dosimetry

Thermoluminescent dosimeter (TLD) is a solid state systems of integrating type dosimeters. Lithium fluoride (LiF) is the most popular material for TLD. It has a regular crystalline structure, when such a crystal is irradiated, a very minute fraction of the absorbed energy is stored in the crystal lattice. Some of this energy can be recovered later as visible light if the material is heated. This phenomenon of the release of visible photons by thermal is known as thermoluminescence (TL)(14).

When the material is irradiated the energy is absorbed from the radiation beam ; some of the electrons of the crystals of LiF are raised to higher energy levels. Most of the electrons immediately return to the ground state but a few remain trapped in the impurity levels. Upon subsequent heating of the LiF, these trapped electrons are elevated to higher electron levels from which they can return to the ground state with the emission of light. The total amount of light emitted will be proportional to the number of electrons that were trapped and it is proportional to the amount of energy absorbed from the radiation (18). A plot of thermoluminescence against temperature or the light output as a function of time is called a glow curve. The different peaks is correspond to different "trapped" energy levels. The area under the whole glow curve can be used to measure dose (18). The emitted light is measured by a photomultiplier tube (PMT) which converts light into an electrical current. The current is then amplified and measured by a recorder or a counter.

LiF : Mg : Ti is commercially available as TLD-600, TLD-700 and TLD-100 containing different amounts of ^{6}Li and ^{7}Li isotopes.

There are ^{6}Li 7.5% for TLD-100, 0.01% for TLD-700 and 95.6% for TLD-600. The relatively high thermal neutron responses of TLD-600 and TLD-100

Copyright by Mahidol University

compared with that of TLD-700 are due to the high absorption cross section of the ^{6}Li nucleus (18).This reaction dominates the neutron response of all phosphors containing ^{6}Li and TLD-100 and TLD-700 are normally used for photon measurement.

The precision of TLD and dose range that the LiF may be used to measure dose over a very wide range from 10^{-5} Gy to 10^{3} Gy (18).

TLD has proved a useful for the measurement of absorbed dose in phantoms and in vivo measurements of radiotherapeutic absorbed dose. Because of their small size also give good spatial resolution.

A complete cycle of use of a TL dosimeter consists of a combination of annealing, storage and handing, calibration and readout.

2.3.1 Annealing.

To ensure complete readout of stored signal and repeated use of the phosphor without significant change in its thermoluminescence sensitivity, a thermal anneal is required. All dosimeters should be identically annealed before making radiation measurement. In order to remove all residual TL signal, to establish the TL sensitivity and to eliminate unstable low temperature glow peaks (19).

The heating programs consist of annealing and preheating (pre-read annealing) before reading.

Annealing : heating to 400°C to one hour and followed by cooling to100°C for two hours and cooling to 45°C.

Preheating : heating to 100°C for ten minutes and cooling to 45°C (20).

Copyright by Mahidol University

2.3.2 Storage and handling

The storage and handling of dosimeter can affect their TL sensitivity, stability, precision and minimum detectable dose. The major effects can be broadly divided due to : (19).

(1). Environmental factors such as temperature, humidity, ultraviolet and visible radiation, etc.

The UV radiation may have an effect in increasing both the background and fading, therefore the dosimeters should be stored in the dark.

(2). Physical handling factors such as dispensing, picking up, cleaning, sterilizing, etc.

It is essential that TLD materials do not become contaminated, especially with grease. They must not be touched by hand.

2.3.3 Calibration

Calibration irradiation, this is carried out to determine the TL response of the dosimeter to a measured exposure or absorbed dose of clearly defined energy. A ^{60}Co source (gamma energies 1.17 and 1.33 MeV, half-life 5.3 years) is most often used for this purpose.

The purpose of calibrating a TLD instrument is to produce consistent and accurate reading in dosimetrically meaningful units.

As the dosimeter is heated and give off light, the photomultiplier tube converts the TL light to electrical current. This current produce a charge integral, expressed in nanocoulombs (nC). This integral is converted to dosimetric units by the Reader Calibration Factor (RCF) ; nC /mR.

Copyright by Mahidol University

A second calibration factor that is the Element Correction Coefficient (ECC), compensates for the variation in sensitivity among dosimeters. In a new installation, the calibration process occurs in three steps : (21).

(1). Generate Calibration Dosimeters

This section describes the specific steps in generating a set of calibration dosimeters. These dosimeters typically 1-2 % of the total population. This process, which generates an Element Correction Coefficient (ECC) for each calibration dosimeter is generally performed only when the instrument and dosimeters are a new installation.

The ECCs for each individual dosimeter are calculated by dividing the average charge integral, <Q> of all the dosimeters by the reading in nC for the individual dosimeter, Q_i .

Let ECC_i be the Element Correction Coefficient for dosimeter i

(i =1,2,3,..,n)

where n is the number of calibration dosimeters :

$$ECC_i = \frac{<Q>}{Q_i} \qquad (4)$$

when < Q > is the average charge integral and given by :

$$< Q > = 1/n \times \sum_{i=1}^{n} Q_i \qquad (5)$$

(2). Calibrate Reader

A subset of these calibration dosimeters is exposed to a known amount of radiation, read with the ECC_i applied and the response of the reader computed in

Copyright by Mahidol University

dosimetric terms "Reader Calibration Factor" (RCF). This process should be chosen calibration dosimeters, that have ECC valves close to 1. The reader calibration factor (RCF) is the ratio of the instrument in nanocoulomb to the actual radiation to which the calibration dosimeters were exposed.

The corrected charge integral, (Q_{ci}) is computed for each dosimeter by.

$$Q_{ci} = Q_i \times ECC_i \quad (6)$$

when Q_i is the reading in nC of each dosimeter and the average corrected charge integral $< Q_c >$, is computed for all the dosimeters and calculated by

$$< Q_c > = 1/n \times \sum_{i=1}^{n} Q_{ci} \quad (7)$$

The RCF is then computed by dividing the average corrected charge integral by the actual absorbed dose, D and given by :

$$RCF = \frac{< Q_c >}{D} \quad (8)$$

(3). Calibrate Dosimeters

This section describes the procedure for generating Element Correction Coefficients (ECC) for each field dosimeter in the system (ECC_{ci}). The dosimeters are exposed to a known radiation, read with the RCF applied, an ECC computed and recorded for each dosimeter.

The system calculates ECCs for each individual dosimeter as follows :

$$ECC_{ci} = \frac{RCF \times L}{Q_{ci}} \quad (9)$$

In which L is the calibration absorbed dose.

Copyright by Mahidol University

2.3.4 Read out

The basis of TL dosimetry is the comparison of TL light signals from dosimeters which have been exposed to an unknown absorbed dose of radiation (D), with TL light signals from similar dosimeters which have been given a calibration absorbed dose. The TL reader should be used in a reproducible manner.

The reading of each TLD is converted to absorbed dose in Gy by

$$D = \frac{Q_i \times ECC_{ci}}{RCF} \qquad (10)$$

Copyright by Mahidol University

CHAPTER III

OBJECTIVES

The irradiation techniques which were studied in this project is the two opposed tangential x-ray beams of 6 MV. The wedge filter and asymmetric fields were used to improve the homogeneity of dose in the treated breast and reduction of dose to tissue outside it. The measurement in the phantom and also at the surface of the patients were performed to:

1. compare the dose distribution of breast in symmetric beams and asymmetric beams by half-beam block with the effect of wedge filter.

2. determine the peripheral doses in chest wall and lung which depends on the effect of treatment techniques.

3. determine the surface dose of target breast and contralateral breast by measuring in the rando phantom.

4. determine the surface dose of target breast and contralateral breast by measuring in the patients.

Copyright by Mahidol University

CHAPTER IV

MATERIALS AND METHODS

4.1 Materials

4.1.1 Therapy unit

The linear accelerator used in the experiment is Clinac 1800 as shown in Fig. 8. This machine produces 6 and 10 MV x-rays beams and five electron energies ranging from 6, 9, 12, 16 and 20 MeV. Its independent collimator system provides the ability to control motion of the upper set of field defining collimators either in an independent or in a symmetric mode of operation. Each upper collimator may be moved passing the beam center while it is in the independent mode. The maximum field size is limited to 40×40 cm^2 at 100 cm source-axis distance in symmetric mode . Its half-beam block side is maximum at 20 cm.

4.1.2 Alderson Rando Phantom

The Alderson rando phantom shown in Fig. 9 incorporates materials to simulate various body tissues-muscle, bone, lung and air cavities. The phantom is shaped into a human torso and is sectioned transversely into slices of 2.5 cm each containing a matrix of 0.5 cm diameter holes spaced 3 cm apart. It is made of tissue-equivalent material based on a synthetic isocyanate rubber. The phantom material is processed chemically and physically to achieve a density of 0.985 g/cm^3 and an effective atomic number of 7.3, based on the International Commission on Radiation

Copyright by Mahidol University

Protection and Measurement. The lungs are molded of an air-expanded version of the soft tissue material having a density of 0.3 g/cm^3 and an effective atomic number is the same as soft tissue.

4.1.3 Thermoluminescent dosimeters, Lithium Fluoride (TLD-100)

The TLD chips have been used in this experiment are Lithium fluoride (LiF) crystals doped with magnesium and titanium (LiF : Mg, Ti) known as TLD 100. The TLDs have a nominal density of 2.64 g/cm^3 and effective atomic number Zeff = 8.2, a value close to tissue. All chips have the surface area of 3.2×3.2 mm^2 and a thickness of 0.89 mm from Harshaw Chemical Company.

4.1.4 Thermoluminescent dosimetry system

The Harshaw Model 5500 Automatic TL Reader in Fig. 10 is a PC-driven, table-top instrument for thermoluminescent dosimetry (TLD) measurement. This reader is capable of reading 50 dosimeters per loading and accommodates TL chips, rods, and cubes in a variety of sizes. The flexible design of the controlling software enables the user to configure the workstation for different applications. The software provides real-time monitoring of the instrument's operating conditions and display of the glow curves and response values. The reader uses hot nitrogen gas heating with a closed loop feedback system that produces linearly ramped temperatures accurate within ± 1°C to 400°C. The Photomultiplier Tube (PMT) Assembly is cooled to a constant temperature maintain consistent performance of the PMT. Nitrogen is routed through the PMT chamber to eliminate condensation.

Copyright by Mahidol University

Fig. 8 The Clinac 1800 linear accelerator.

Copyright by Mahidol University

Fig. 9 The Alderson Rando Phantom.

Copyright by Mahidol University

Fig. 10 The Harshaw model 5500 Automatic TL Reader.

Copyright by Mahidol University

4.2 Methods

This experiment was carried on into three steps:

- TLD calibration
- Determination of the absorbed dose at the interesting points in the rando phantom
- Measurement of surface dose in the patients.

4.2.1 TLD calibration

Thermoluminescent dosimeters (TLDs), TLD-100 chips with the automatic TL reader of the Harshaw model 5500 were used to measure the radiation doses at various points in the phantom and the patient. Before using TLDs for dose measurement, all TLDs of 120 chips were annealing and irradiation of 100 cGy for ten times. After excited, TLDs were calibrated to determine the ECC and RCF for each individual dosimeter with gamma rays from THERATRON 780 cobalt-60 teletherapy machine of 100 cGy, FS 10×10 cm^2 at SSD 80 cm.

To confirm the constancy of TLD, on the same day of each measurement, five reference TLDs were irradiated in solid water phantom to 100 cGy of 6 MV x-ray at the depth of maximum dose (1.5 cm), field size 10×10 cm^2 and source to surface distance 100 cm. Reference TLDs were read after irradiated.

4.2.2 Determination of the absorbed dose at the interesting point in rando phantom

The absorbed dose in breast, chest wall, lung, surface and contralateral breast were measured throughout the breast rando phantom at 2.5 cm interval along the axis of the phantom, the slabs used were number 15^{th} to 19^{th} (Fig. 11 to16). Three TLD chips were loaded in a plastic capsule which were placed in the holes of the rando phantom.

Copyright by Mahidol University

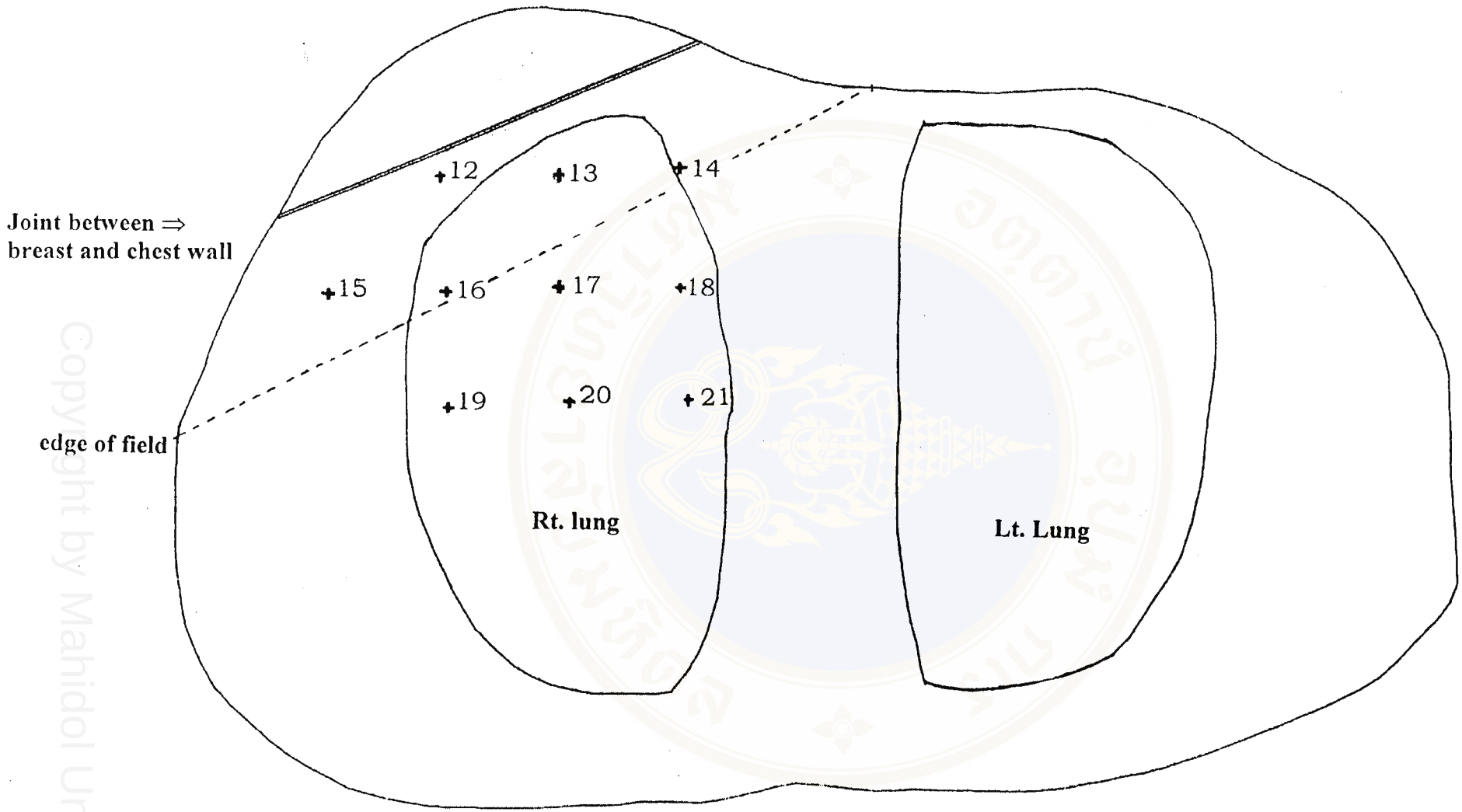

Fig. 11 The absorbed dose measurement at various points in the 15th slab of the rando phantom in symmetric and asymmetric beams.

Copyright by Mahidol University

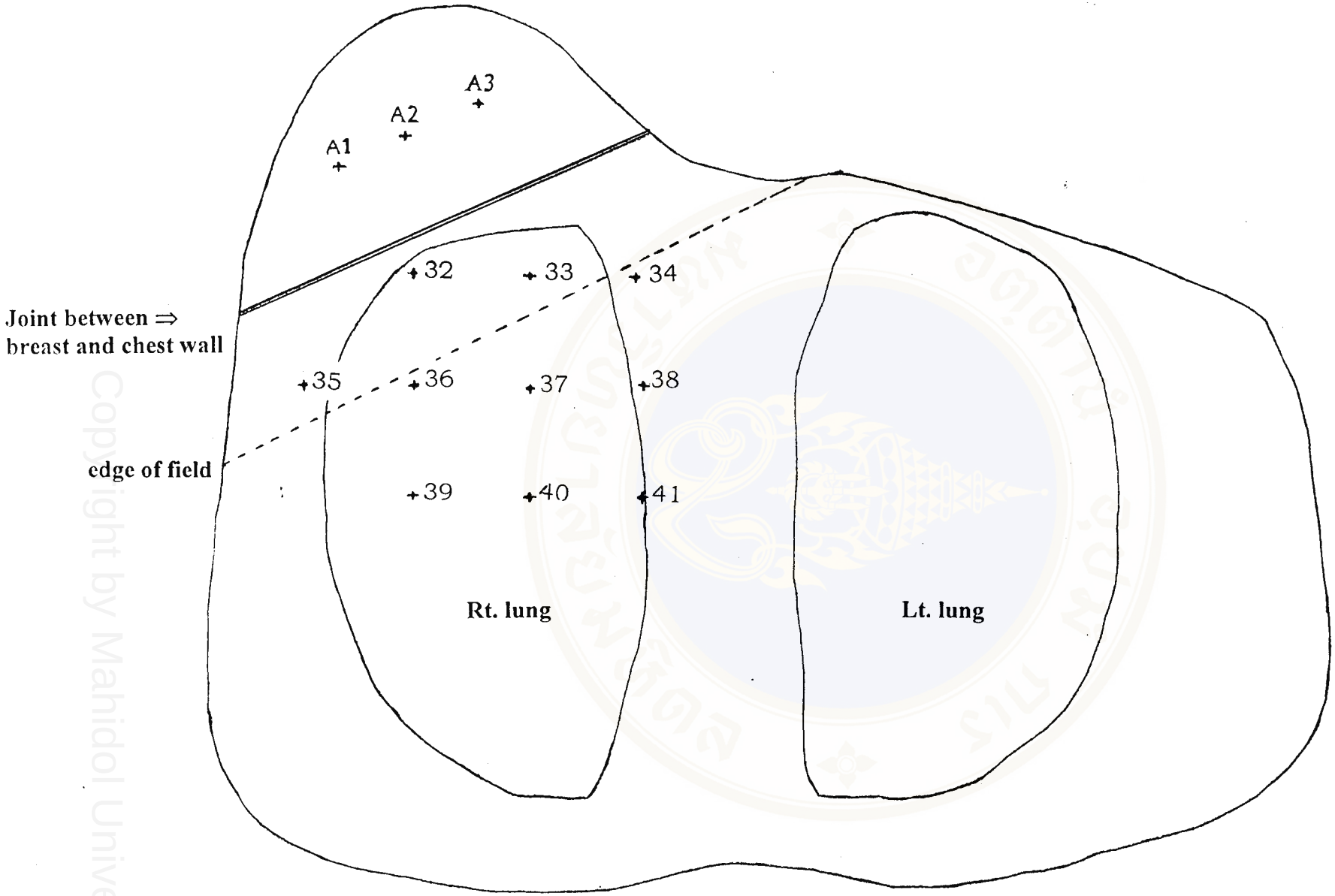

Fig. 12 The absorbed dose measurement at various points in the 16th slab of the rando phantom in symmetric and asymmetric beams.

Copyright by Mahidol University

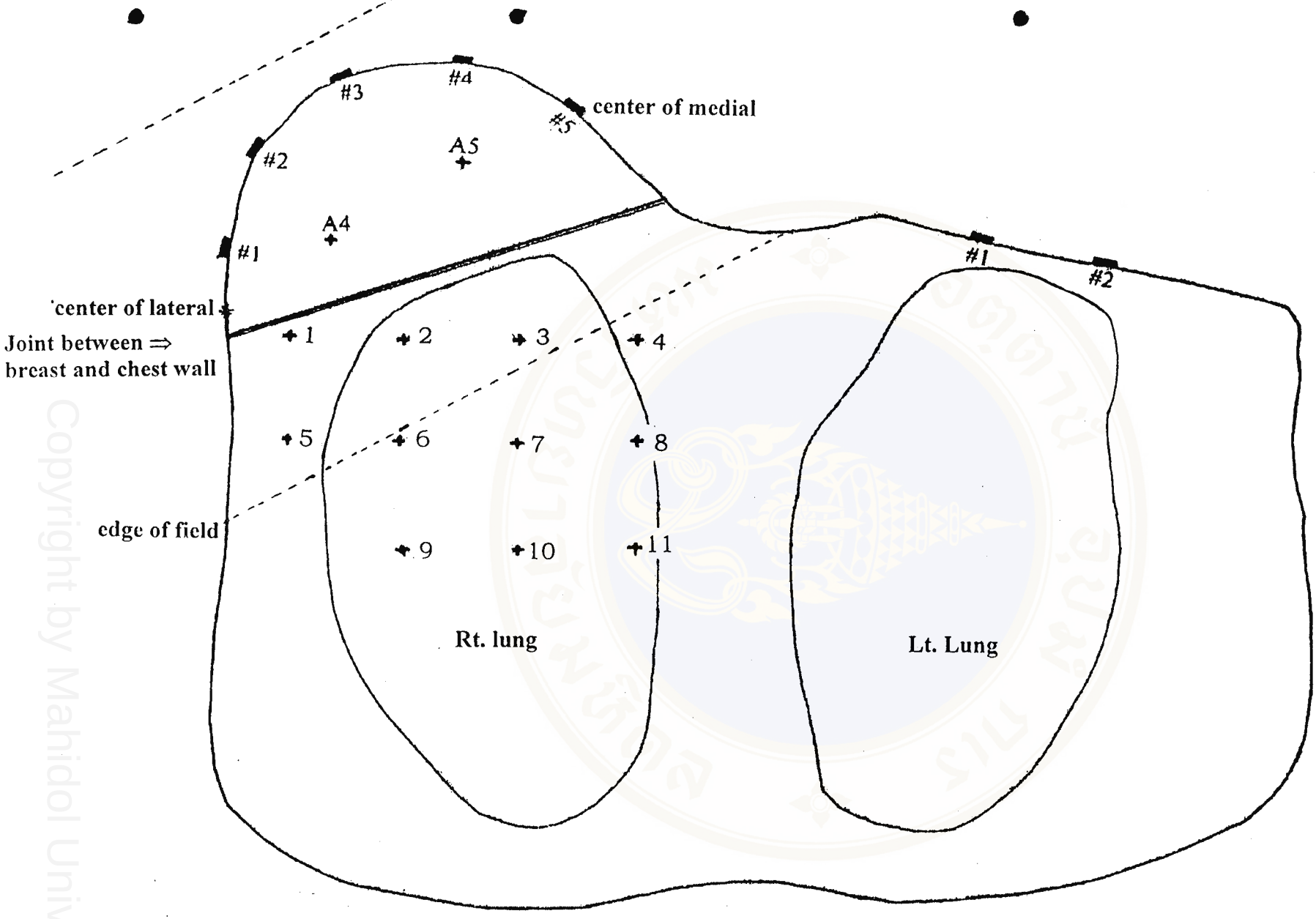

Fig. 13 The absorbed dose measurement at various points in the 17th slab of the rando phantom in symmetric and asymmetric beams.

Copyright by Mahidol University

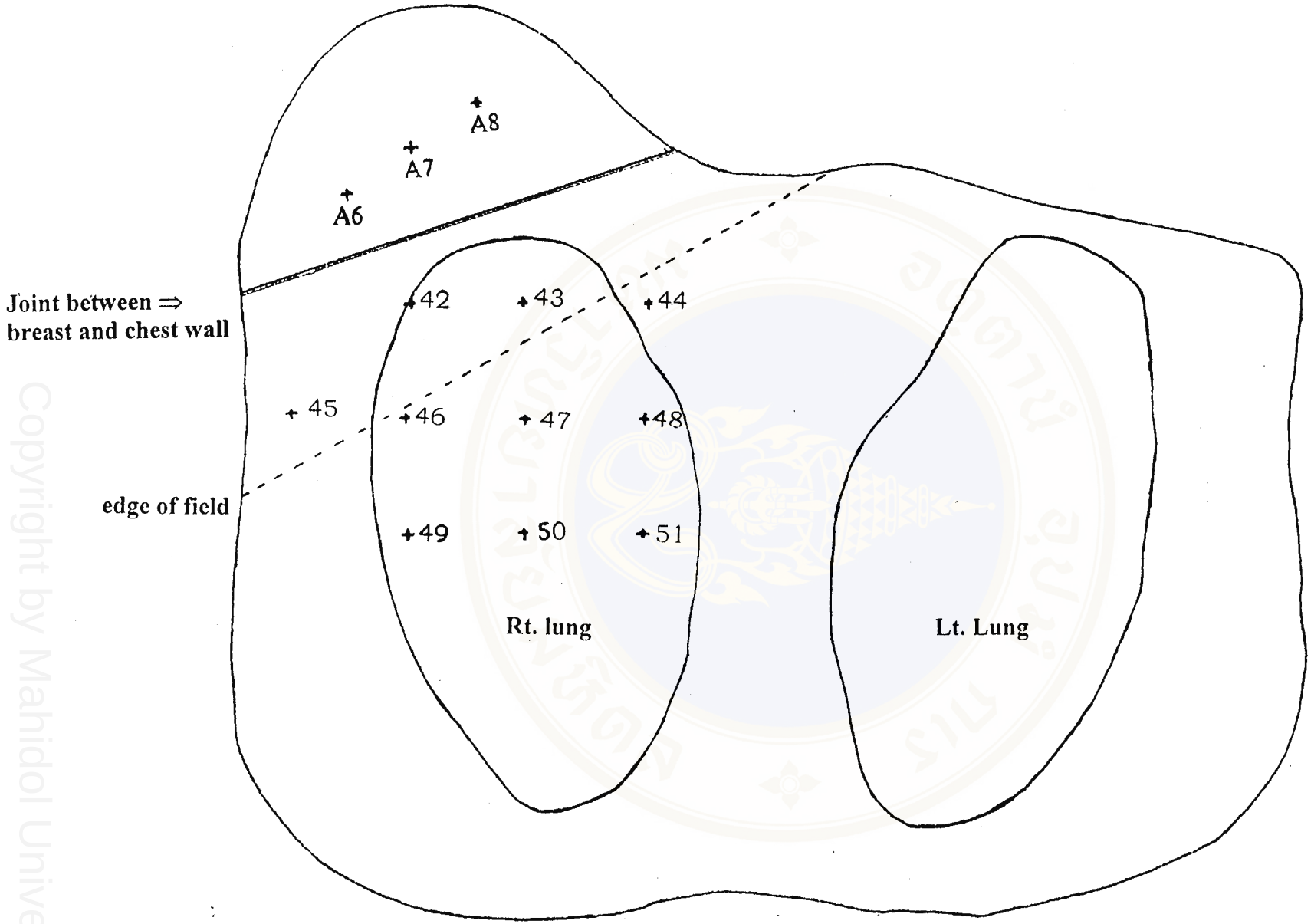

Fig. 14 The absorbed dose measurement at various points in the 18th slab of the rando phantom in symmetric and asymmetric beams.

Copyright by Mahidol University

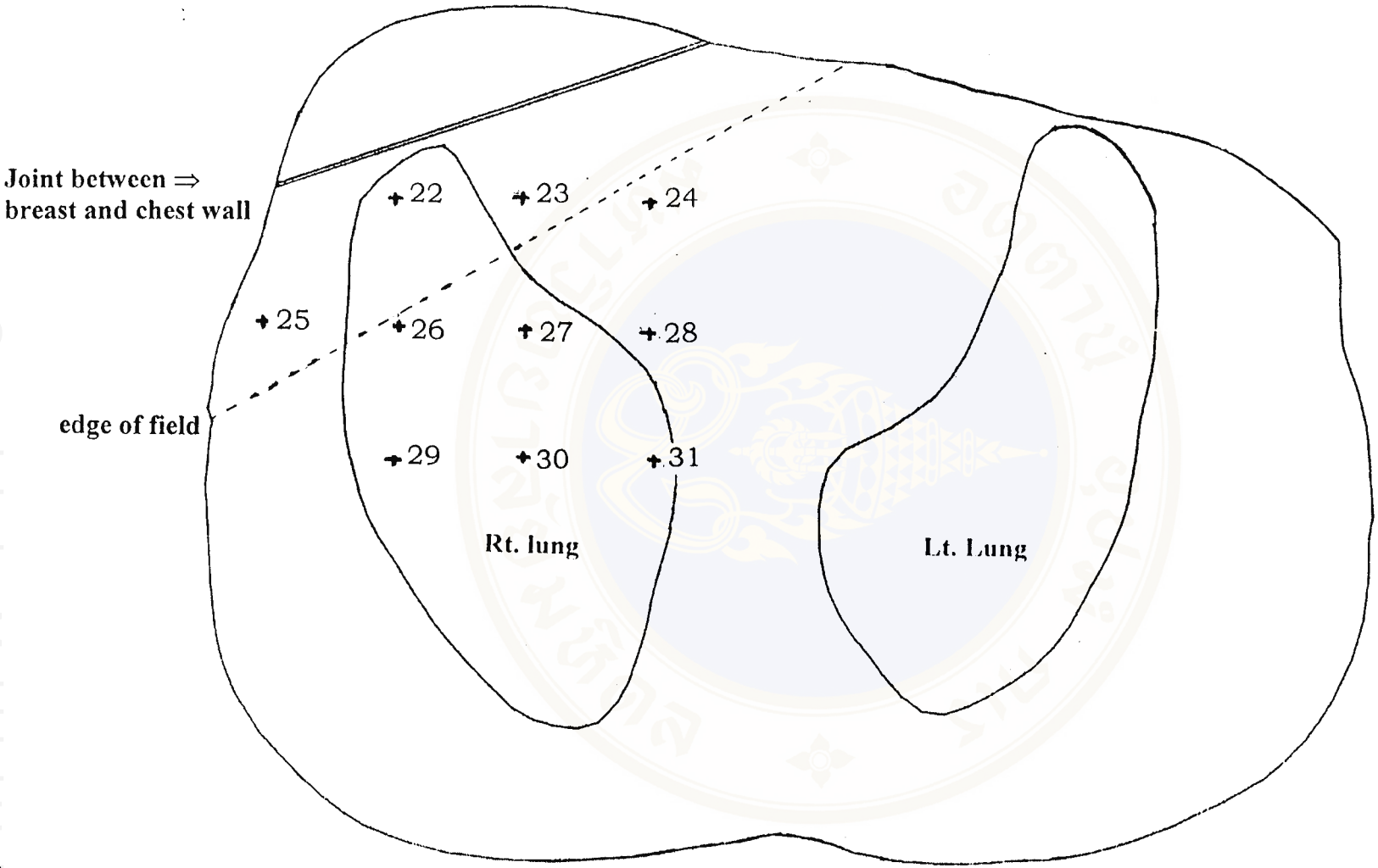

Fig. 15 The absorbed dose measurement at various points in the 19th slab of the rando phantom in symmetric and asymmetric beams.

293627 i 11782018

Copyright by Mahidol University
LIBRARY AND INFORMATION CENTER
MAHIDOL UNIVERSITY

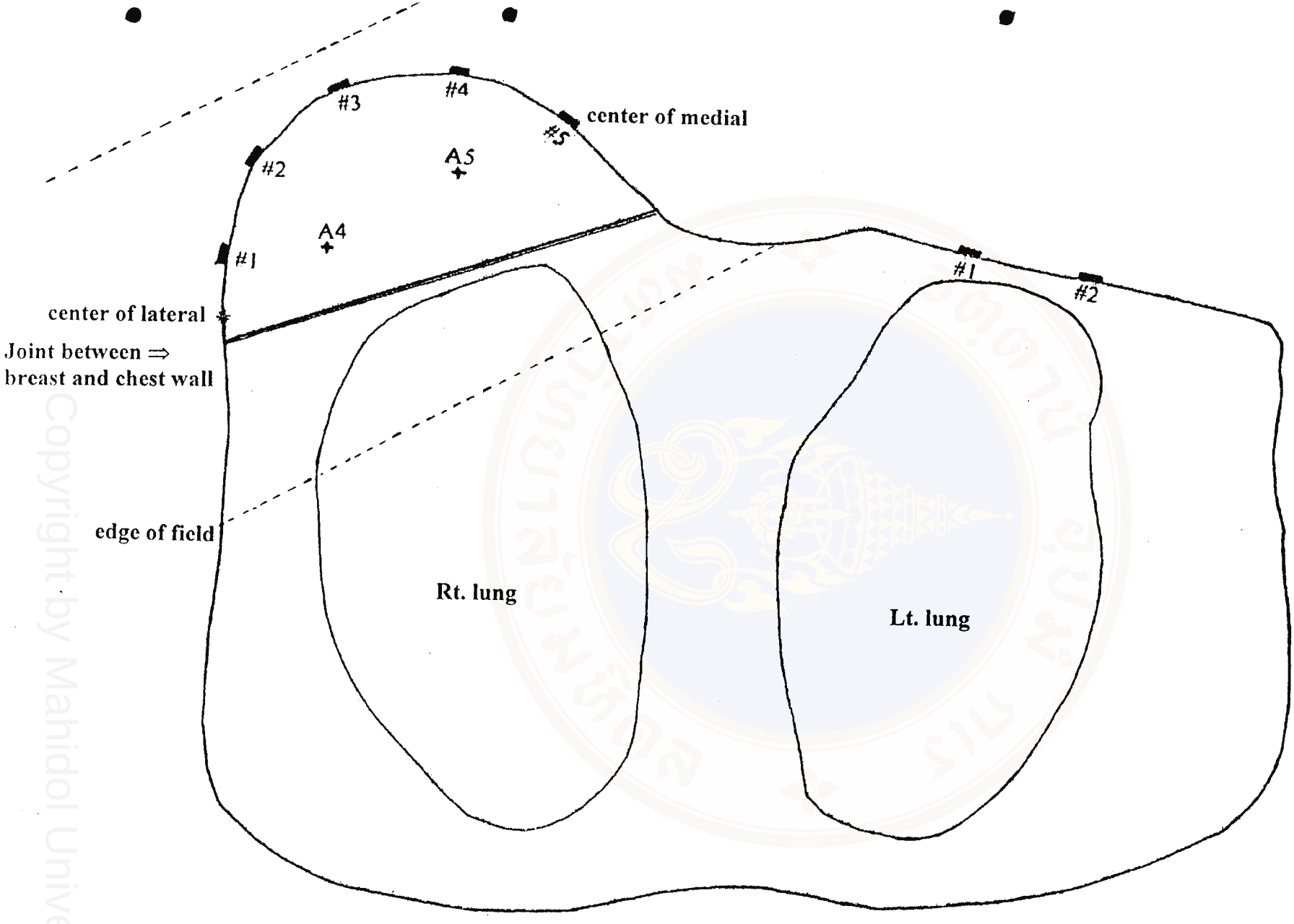

Fig. 16 The surface dose measurement at various points on the target and contralateral breast of the rando phantom in symmetric and asymmetric beams.

Copyright by Mahidol University

Two irradiation techniques were evaluated, the first technique was the SSD symmetric beam, the second used the SSD asymmetric beam. For each technique the open beam , 15 and 30 degree wedge were used for medial and lateral fields.

For each technique open beam and wedge configuration, three measurements were made, and the TLD readings were averaged.

The field size 10.5×18 cm^2 was used to covered the treated breast. The average maximum extension of lung in the beam was about 2.5 cm measured perpendicularly from the posterior beam edge.

The absorbed dose of 100 cGy were given at the reference point which was the average value at point A_4 and A_5 in fig.13.

(A) Symmetric beam technique (Fig. 17)

The irradiation of tangential fields were performed by setting the chest rando phantom with one breast intact in supine position. The medial and lateral border of the tangential breast fields were marked which similar to the real treatment of the patient. The set up was performed by the simulators. The center of the beams were arranged in such a way that the lower edge of the beams passed through the marked border. The source to surface distance was 100 cm. The gantry angles were 60 degree and 210 degree for medial and lateral field, respectively. The field size was 10.5×18 cm^2. The collimator and couch rotation were 0 degree.

Copyright by Mahidol University

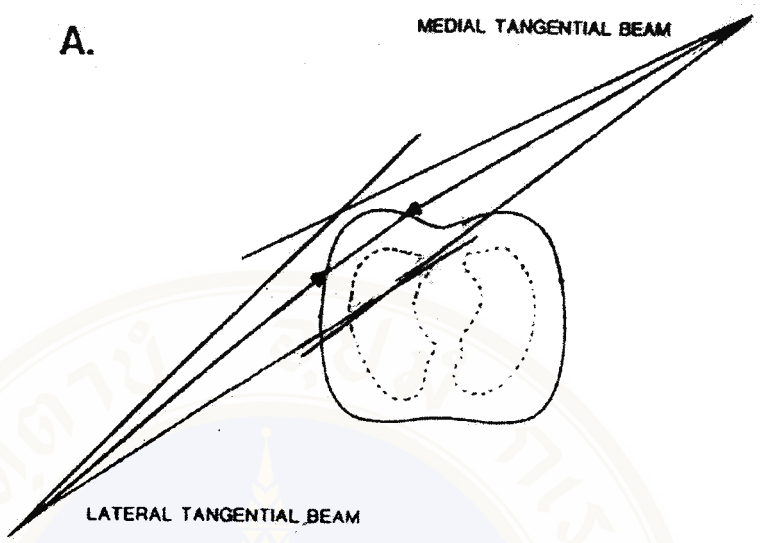

Fig. 17 Symmetric beam technique of tangential fields.

(B) Asymmetric beam technique (Fig. 18)

The irradiation technique with two oblique tangential fields were used with SSD-technique of 100 cm. The central axis of the beam was set along the edge of field. The gantry angle and couch rotation for this technique were the same as the symmetric beam technique. But the collimator rotation was 270 degree and the field size of asymmetric mode was 10.5×18 cm^2. The medial and lateral fields were set asymmetric in Y jaws with Y2 set to 0.0 and Y1 set to 10.5 cm and the X jaws set to the longitudinal length.

Copyright by Mahidol University

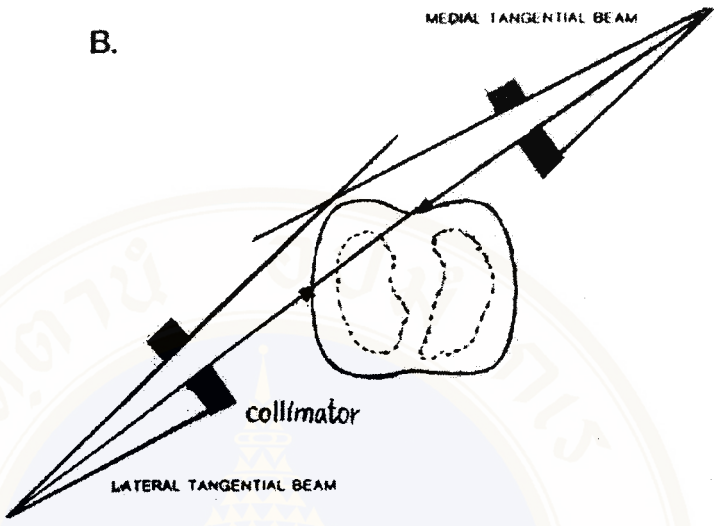

Fig. 18 Asymmetric beam technique of tangential fields.

4.2.3 Measurement of the surface dose in the patients

1) measurement of surface dose to target breast

2) measurement of surface dose to contralateral breast

In this study the patients were selected to be treated with breast conservation therapy. The dimension of the patients were in the average dimension of the rando phantom. The patients were treated with opposing tangential breast irradiation with SSD-technique of 6 MV x-rays beam in Clinac 1800 linear accelerator. The tumor dose is 200 cGy per day. The irradiation techniques consist of open beam and wedge beams (15, 30 degree) in both of symmetric beam and asymmetric beam by half-beam block. To compare the various techniques used, one patient was treated using open beam , 15 and 30 degree wedges.

Copyright by Mahidol University

For each dose measurement, three TLD chips were loaded in plastic capsule and placed on the patient's surface of the target breast. The five TLD capsules were employed to measured the surface dose along the transverse central axis plane as shown in Fig. 19. Two TLD capsules were placed on the contralateral breast which one was 5 cm lateral from the edge of the medial tangential field and the other one was near the nipple. TLD measurements were performed 2 times for each technique about one week separation.

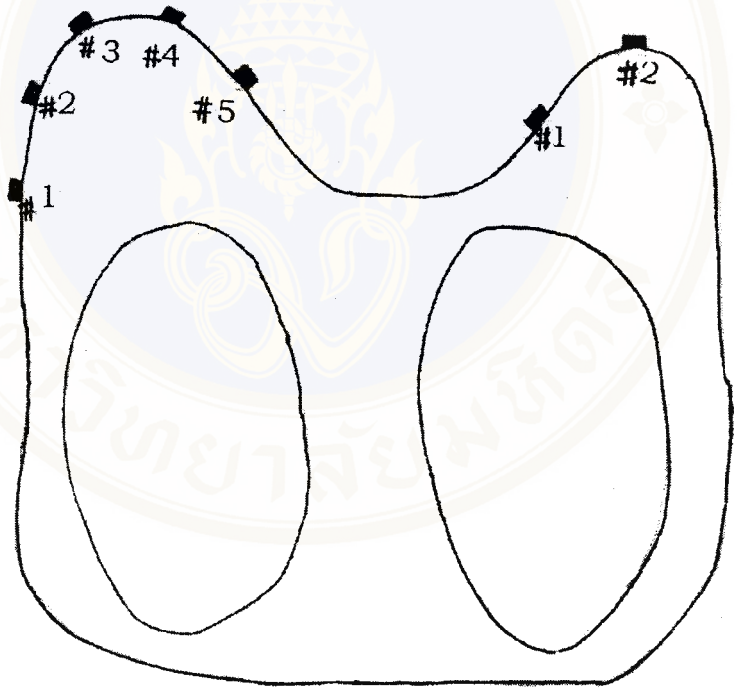

Fig. 19 The TLD position on surface of target and contralateral breast on the patients.

Copyright by Mahidol University

CHAPTER V

RESULTS

5.1 Results

5.1.1 TLD calibration

After the ECC and RCF values were determined, the precision for a group of TLD chips was tested by measuring the TL response and then the standard deviation was calculated. The reading of the TLD chips were evaluated using the sensitivity values for each chip to establish a dose reading relative to the standard. The measurement gave the mean values 100 cGy and standard deviation 3.96%.

Five calibrated TLD chips were confirmed to check the constancy. The measurement gave the mean values of 100.79 cGy and standard deviation 3.47%.

To confirm the accuracy of this study, 3 TLD chips were irradiated in each measurement points and the measurement were repeated three times. A reading gave the average of dose at that point. For each measurement, the calibrated TLD were irradiated with known of 100 cGy, the deviation from prescribed dose was corrected. The TLD reading for repeated measurement on the same geometry were reproducible within ± 10%.

Copyright by Mahidol University

5.1.2 Determination of the absorbed dose at the interesting points in rando phantom

1) The absorbed dose measurement in the breast phantom

The measurement points in the breast phantom in three transverse planes which are 2.5 cm separation are shown in Fig. 20. The arrangement of measurement points into coronal plane are shown in Fig. 21. The absorbed dose measurement at various points in the breast phantom in the mid coronal plane for symmetric and asymmetric beams are shown in Table 1 and 2.

The prescribed dose is 200 cGy, point A_4 and A_5 are the reference points which was given 200 cGy. The results in Table 1 and 2 show the agreement between calculated value and the average measured dose with the maximum difference of 4.03%.

The data from Table 1 and 2 are plotted and shown in Fig. 22. The graph shows that the measured dose at point A_3, A_4 and A_5 of six techniques are closed to 200 cGy, six lines which were shown from point A_1 to A_8 for each technique tend to be come closer when passing through point A_1, A_3, A_4, A_5 and A_6, but the lines are separated wider when passing through the other points. They tend to be deviated from 200 cGy. The absorbed dose at the points in upper plane tend to be higher than 200 cGy but the absorbed dose at the points in lower plane behave in the different way. The line in lower plane of asymmetric beam deviate more downward than the symmetric beam.

Copyright by Mahidol University

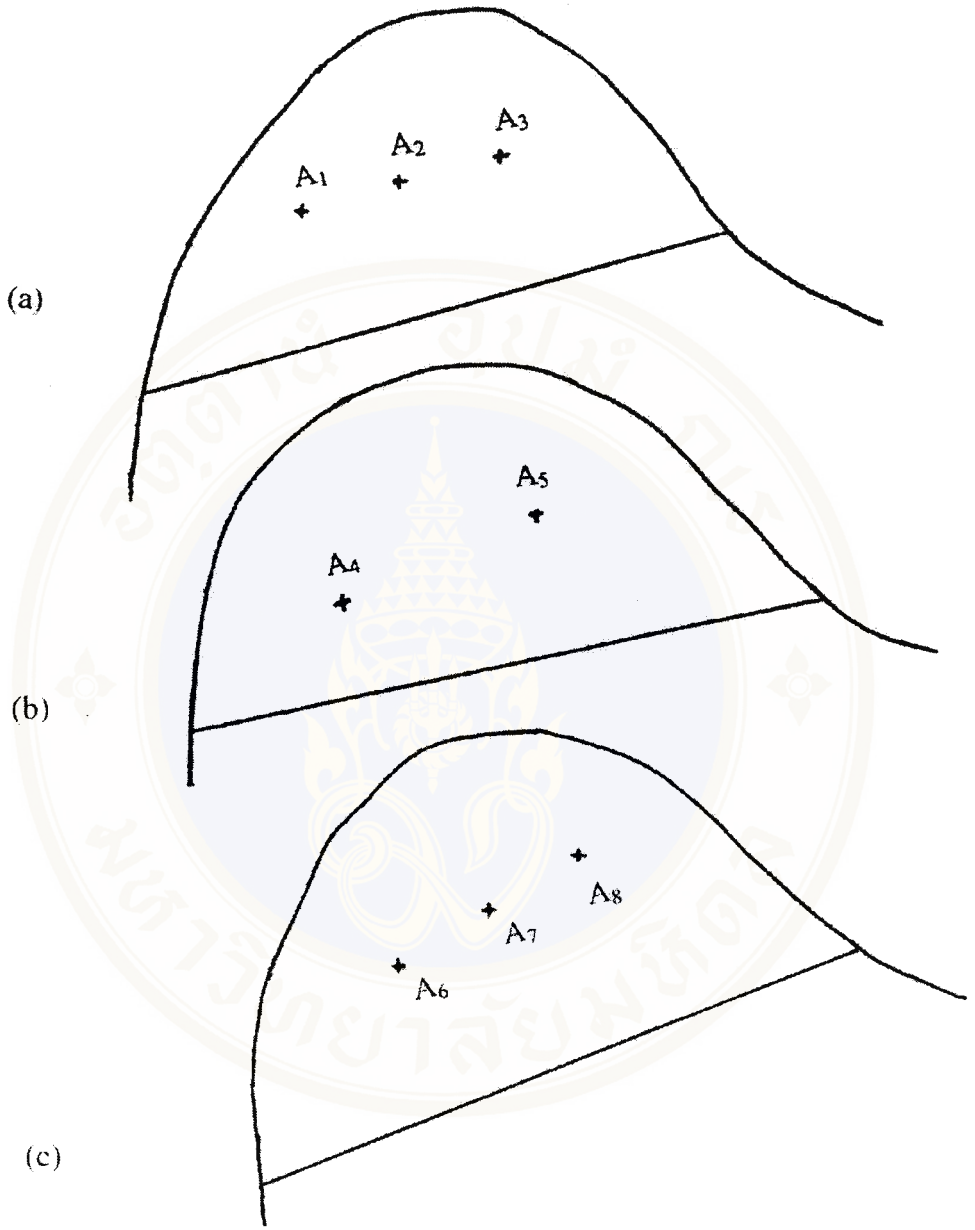

Fig. 20 The various points in the breast phantom in the transverse plane (a) in the 16th slab of rando phantom which is 2.5 cm upper to the center , (b) in the 17th slab which is at the center and (c) in the 18th slab which is 2.5 cm lower to the center, respectively.

Copyright by Mahidol University

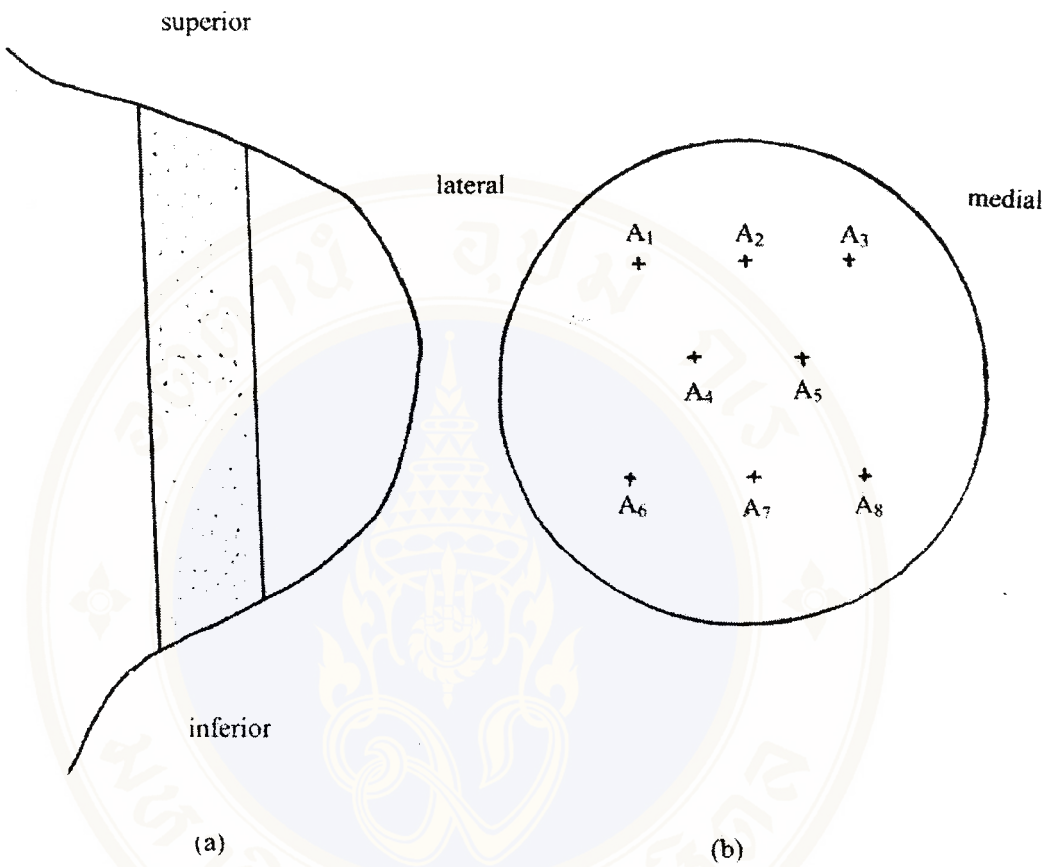

Fig. 21 (a) The region of the mid coronal plane in the breast phantom.

(b) The various points in the breast phantom in the mid coronal plane.

Copyright by Mahidol University

Table 1 The absorbed dose measurement at various points in the breast phantom in the mid coronal plane in symmetric beams.

Point	Dose measurement (cGy)		
	Open beam	Wedge 15°	Wedge 30°
Upper plane			
A_1	209.58	209.46	215.45
A_2	205.51	218.96	223.72
A_3	199.97	208.13	202.91
Central plane			
A_4	211.11	203.73	206.31
A_5	204.98	197.98	196.30
Average	**208.05**	**200.86**	**201.31**
Lower plane			
A_6	198.13	190.27	192.98
A_7	209.63	189.44	185.89
A_8	190.89	181.14	178.25

Table 2 The absorbed dose measurement at various points in the breast phantom in the mid coronal plane in asymmetric beams.

Point	Dose measurement (cGy)		
	Open beam	Wedge 15°	Wedge 30°
Upper plane			
A_1	204.70	205.20	200.45
A_2	208.05	191.83	189.01
A_3	187.58	208.00	207.14
Central plane			
A_4	203.40	216.81	212.13
A_5	185.35	194.38	188.15
Average	**194.38**	**205.60**	**200.14**
Lower plane			
A_6	183.29	186.39	181.09
A_7	171.72	181.76	180.01
A_8	169.28	172.77	174.76

Copyright by Mahidol University

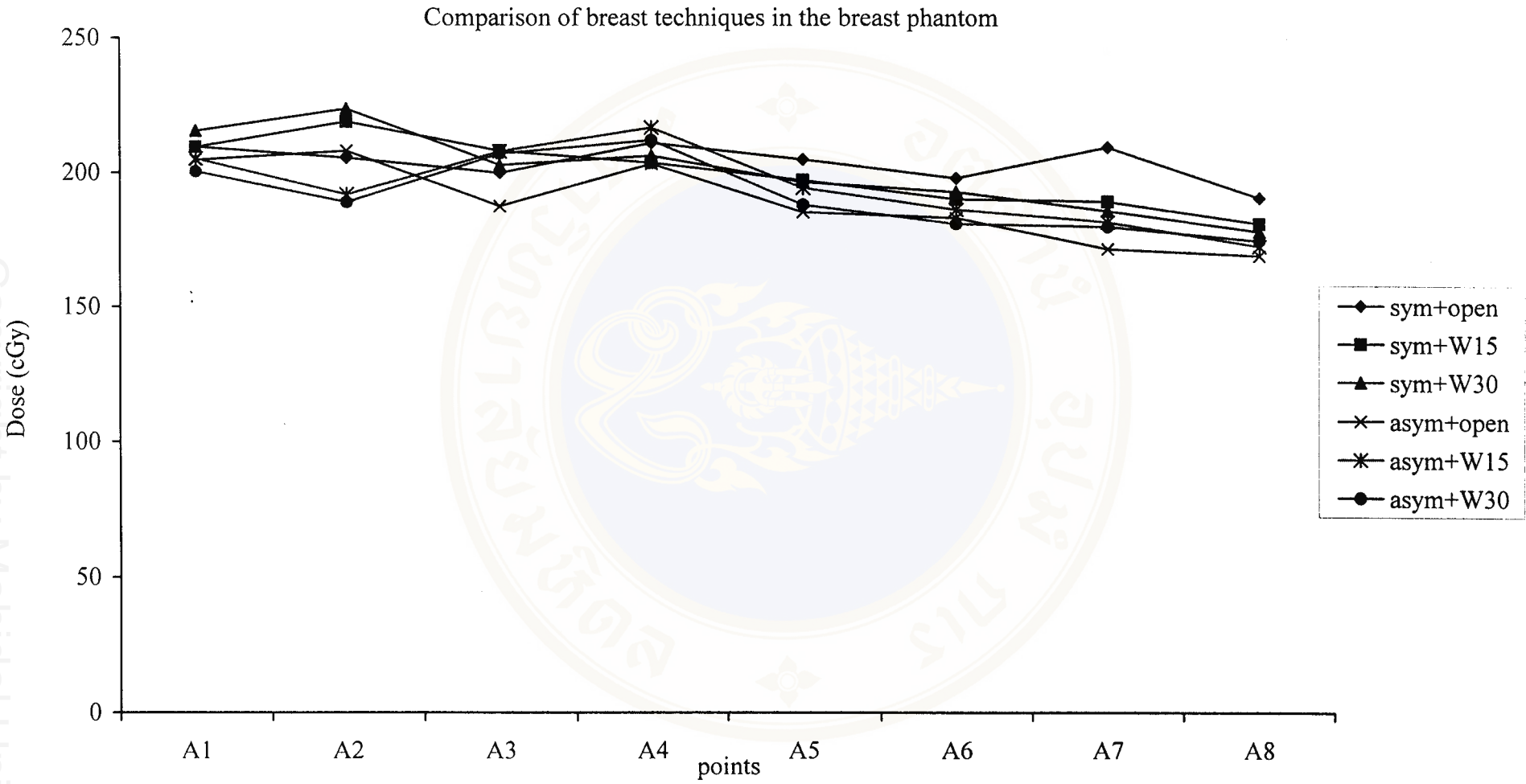

Fig. 22 Comparison of dose at various points in the breast phantom in symmetric and asymmetric beams.

Copyright by Mahidol University

The measurement dosed in table 1 and 2 were normalized to the prescribed dose, there are the percentage relative dose which are shown in table 3. The percentage relative doses in symmetric beams range from 95.45 to 105.56, 90.57 to 109.48, 89.13 to 111.86 for open beam, 15° and 30° wedged beams, respectively. For asymmetric beams, the percentage relative doses range from 84.64 to 104.03, 86.39 to 108.41 and 87.38 to 106.07 for open beam, 15° and 30° wedged beams.

Table 3 The comparison of dose distribution of target breast from different techniques (the percentage relative doses).

Point	The percentage relative doses					
	Sym+open	Sym+W15°	Sym+W30°	Asym+open	Asym+W15°	Asym+W30°
A_1	104.79	104.73	107.73	102.35	102.60	100.23
A_2	102.75	109.48	111.86	104.03	95.92	94.51
A_3	99.99	104.07	101.46	93.79	104.00	103.57
A_4	105.56	101.87	103.16	101.70	108.41	106.07
A_5	102.49	98.64	98.15	92.68	97.19	94.08
A_6	99.07	95.14	96.49	91.65	93.20	90.55
A_7	104.82	94.72	92.95	85.86	90.88	90.01
A_8	95.45	90.57	89.13	84.64	86.39	87.38

Copyright by Mahidol University

1) The absorbed dose measurement in the chest wall and lung

Table 4 and 9 present the results of the absorbed dose measurement at various points in 17^{th}, 15^{th} and 19^{th} slabs of the chest rando phantom which are at the center , 5 cm upper and 5 cm lower to the transverse central plane. To compare the absorbed dose point by point for symmetric and asymmetric beams, the measured dose in chest wall with breast contour are shown in Fig.23 to Fig.31. The results clearly show that the absorbed dose at all points in chest wall and lung in symmetric beams are higher than the absorbed dose in asymmetric beams. The data from table 4 to 9 were arranged in such a way that the measured doses were normalized to the prescribed dose. The dose to chest wall and lung were separated into the point which are in and out of the treatment fields, the data are shown in table 10 and 11.

The chest wall and lung doses are increased with the larger degree of wedge filter used both in symmetric and asymmetric beams, the results are the same for three planes of interest.

In the central plane of the beams, the average percentage relative dose of chest wall in the area of the symmetric beams are 92.00, 95.91 and 101.14 for open beam, 15° and 30° wedged beams, respectively. The average percentage relative dose out of the beams are 20.82, 18.37 and 28.97, respectively. For asymmetric beams, the average percentage relative dose of chest wall in the treatment fields are 85.88, 91.89 and 94.82. The points outside the field give the average percentage relative dose 11.51, 13.72 and 13.86 to open beam, 15° and 30° wedged beams, respectively.

The chest wall doses in the treatment fields for the upper plane are higher than lower plane about 5%, but the dose in lower plane are comparable to those in the central plane.

Copyright by Mahidol University

The average percentage relative lung doses in the central plane of treatment fields range from 87.62 to 99.11 for symmetric beams with open to wedged beams, while they range from 71.42 to 79.13 for asymmetric beams. These results clearly show the advantage of using asymmetric beams. The average percentage relative lung doses out of the field range from 4.09 to 6.44 for symmetric beams with open beam to wedged beams, while they range from 3.54 to 5.14 for asymmetric beams.

Copyright by Mahidol University

Table 4 The absorbed dose measurement at various points in the 17th slab of the chest rando phantom which is the central plane in symmetric beams.

Point	Dose measurement (cGy)		
	Open beam	Wedge 15°	Wedge 30°
1	178.72	192.52	189.03
2	185.88	184.17	201.26
3	185.69	190.25	208.63
4	41.63	36.73	57.93
5	189.28	191.12	215.50
6	154.11	147.67	184.75
7	15.56	17.43	21.82
8	7.71	10.18	11.77
9	8.70	10.40	13.12
10	5.23	8.03	10.42
11	3.67	5.93	7.24

Table 5 The absorbed dose measurement at various points in the 17th slab of the chest rando phantom which is the central plane in asymmetric beams.

Point	Dose measurement (cGy)		
	Open beam	Wedge 15°	Wedge 30°
1	173.37	186.03	189.12
2	170.59	179.15	187.53
3	162.61	171.34	185.25
4	23.00	27.43	27.71
5	172.13	181.50	190.16
6	95.29	89.11	100.02
7	12.97	15.58	15.04
8	6.56	8.70	10.41
9	7.56	8.95	10.50
10	4.63	7.48	8.32
11	3.64	5.53	7.11

Copyright by Mahidol University

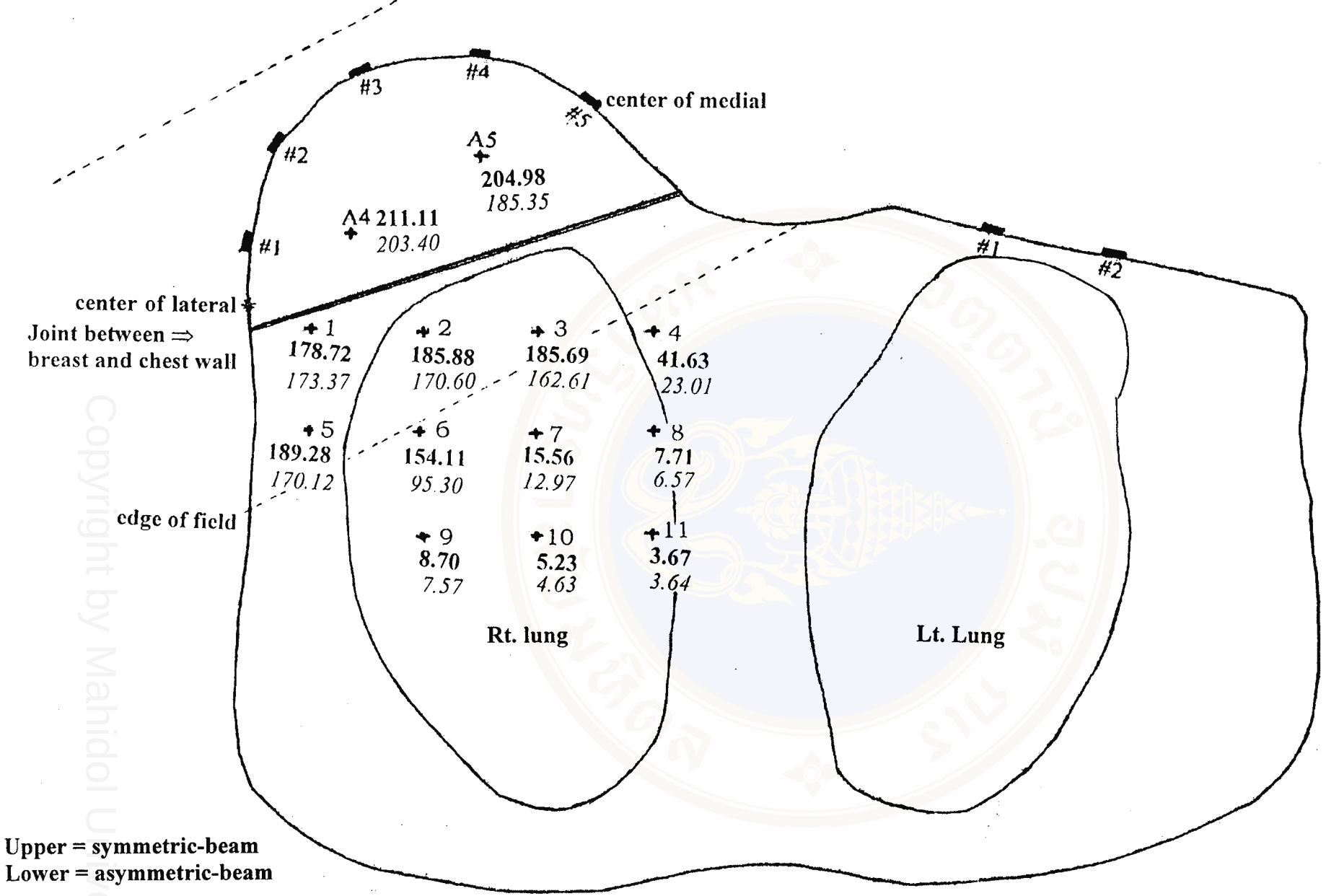

Fig. 23 The absorbed dose measurement at various points in the 17th slab of the rando phantom which is the central plane by open beam technique in symmetric and asymmetric beams.

Copyright by Mahidol University

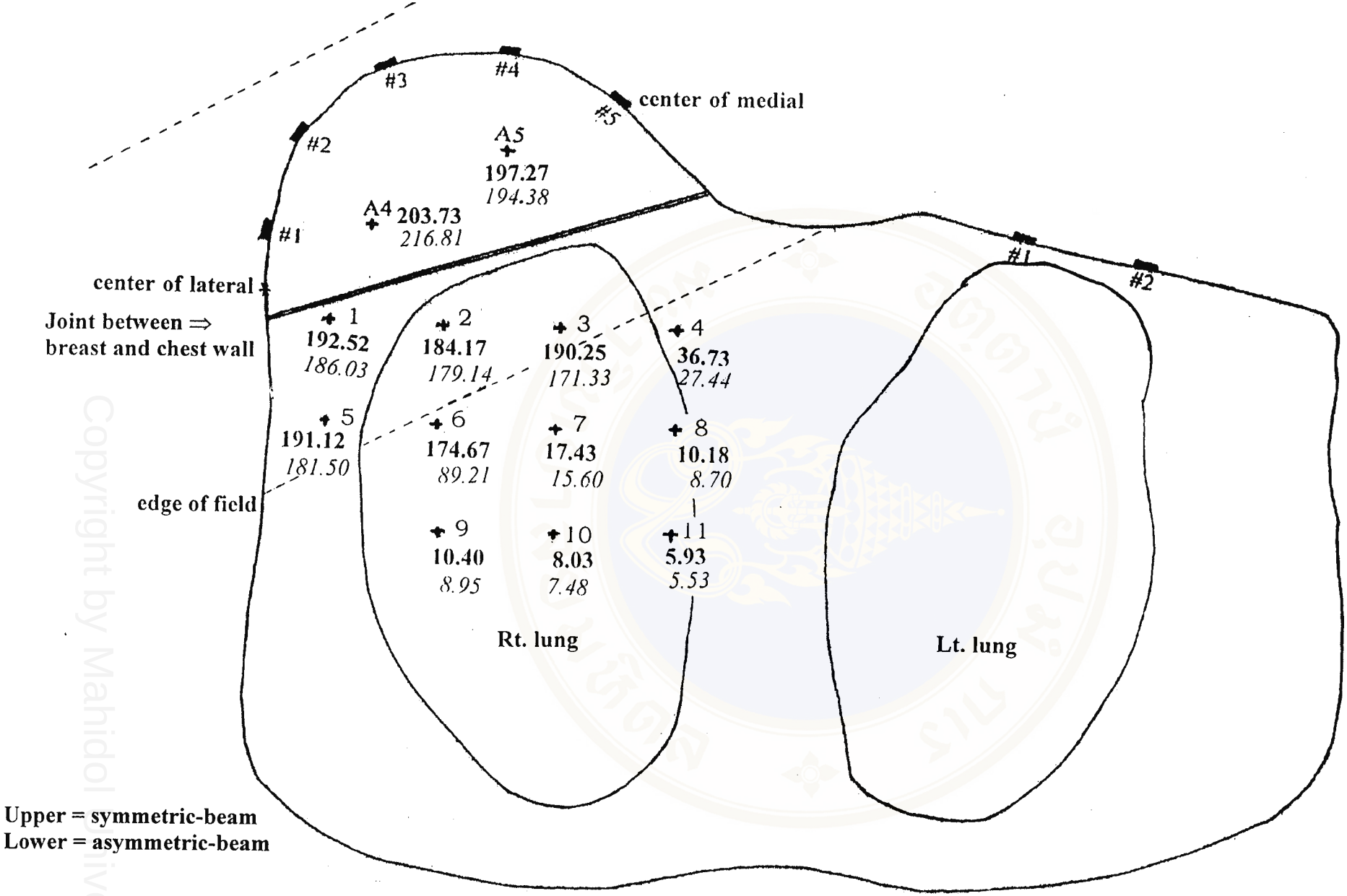

Fig. 24 The absorbed dose measurement at various points in the 17th slab of the rando phantom which is the central plane by 15° wedged beam technique in symmetric and asymmetric beams.

Copyright by Mahidol University

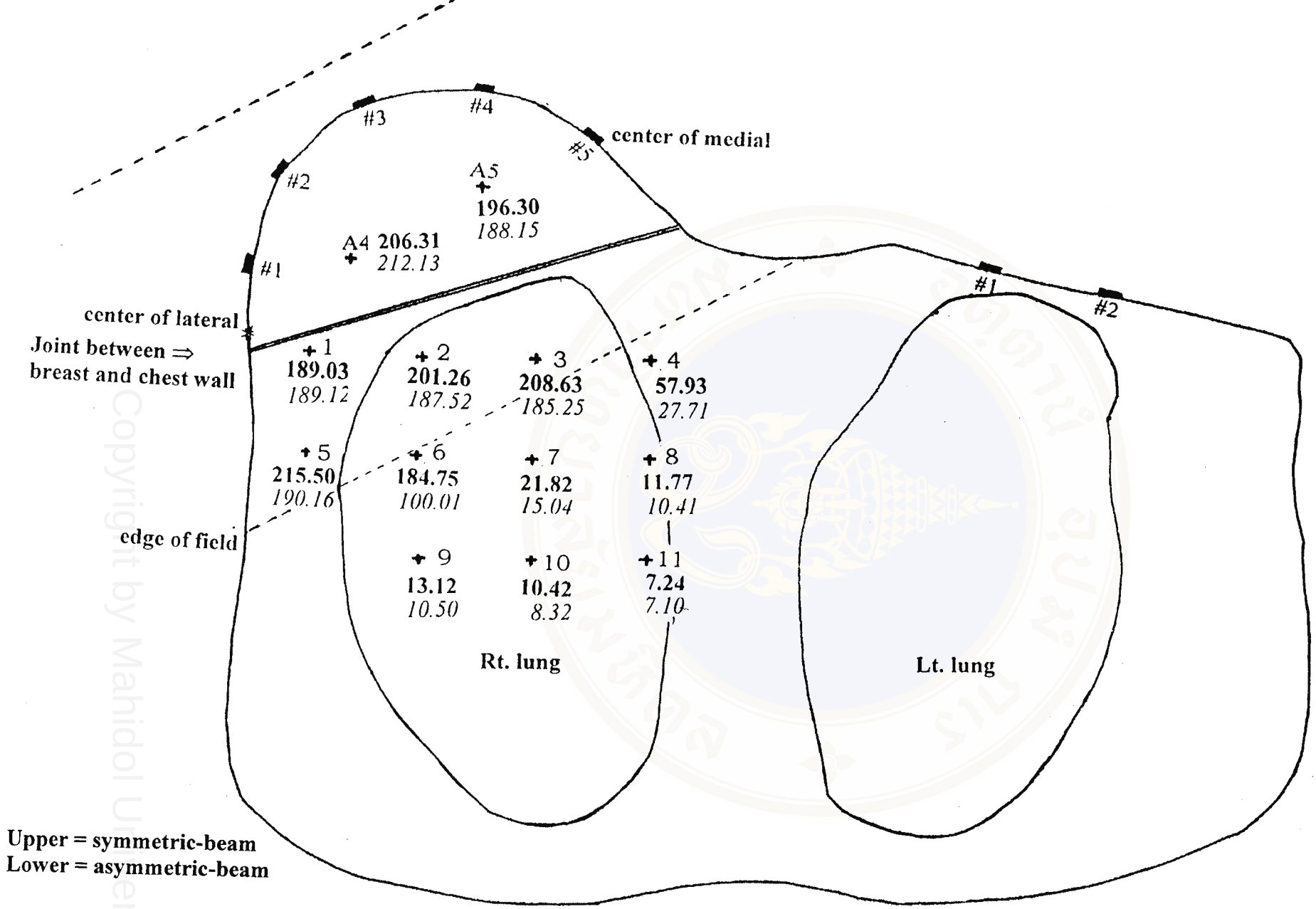

Fig. 25 The absorbed dose measurement at various points in the 17th slab of the rando phantom which is the central plane by 30° wedged beam technique in symmetric and asymmetric beams.

Copyright by Mahidol University

Table 6 The absorbed dose measurement at various points in the 15th slab of the chest rando phantom which is 5 cm upper off axis from the central plane in symmetric beams.

Point	Dose measurement (cGy)		
	Open beam	Wedge 15°	Wedge 30°
12	194.05	199.11	225.18
13	200.80	202.21	234.98
14	183.44	131.09	137.57
15	198.76	207.94	226.14
16	179.01	181.76	189.99
17	22.63	23.79	30.02
18	7.95	10.25	13.11
19	9.73	11.66	15.23
20	5.79	8.10	10.41
21	3.86	6.04	7.45

Table 7 The absorbed dose measurement at various points in the 15th slab of the chest rando phantom which is 5 cm upper off axis from the central plane in asymmetric beams.

Point	Dose measurement (cGy)		
	Open beam	Wedge 15°	Wedge 30°
12	192.31	197.78	201.67
13	184.35	190.31	195.81
14	85.57	113.35	69.33
15	188.55	207.49	214.32
16	155.33	151.15	128.19
17	16.22	21.44	21.47
18	7.80	8.97	10.44
19	7.45	10.95	12.04
20	5.61	7.04	8.63
21	3.63	5.48	6.75

Copyright by Mahidol University

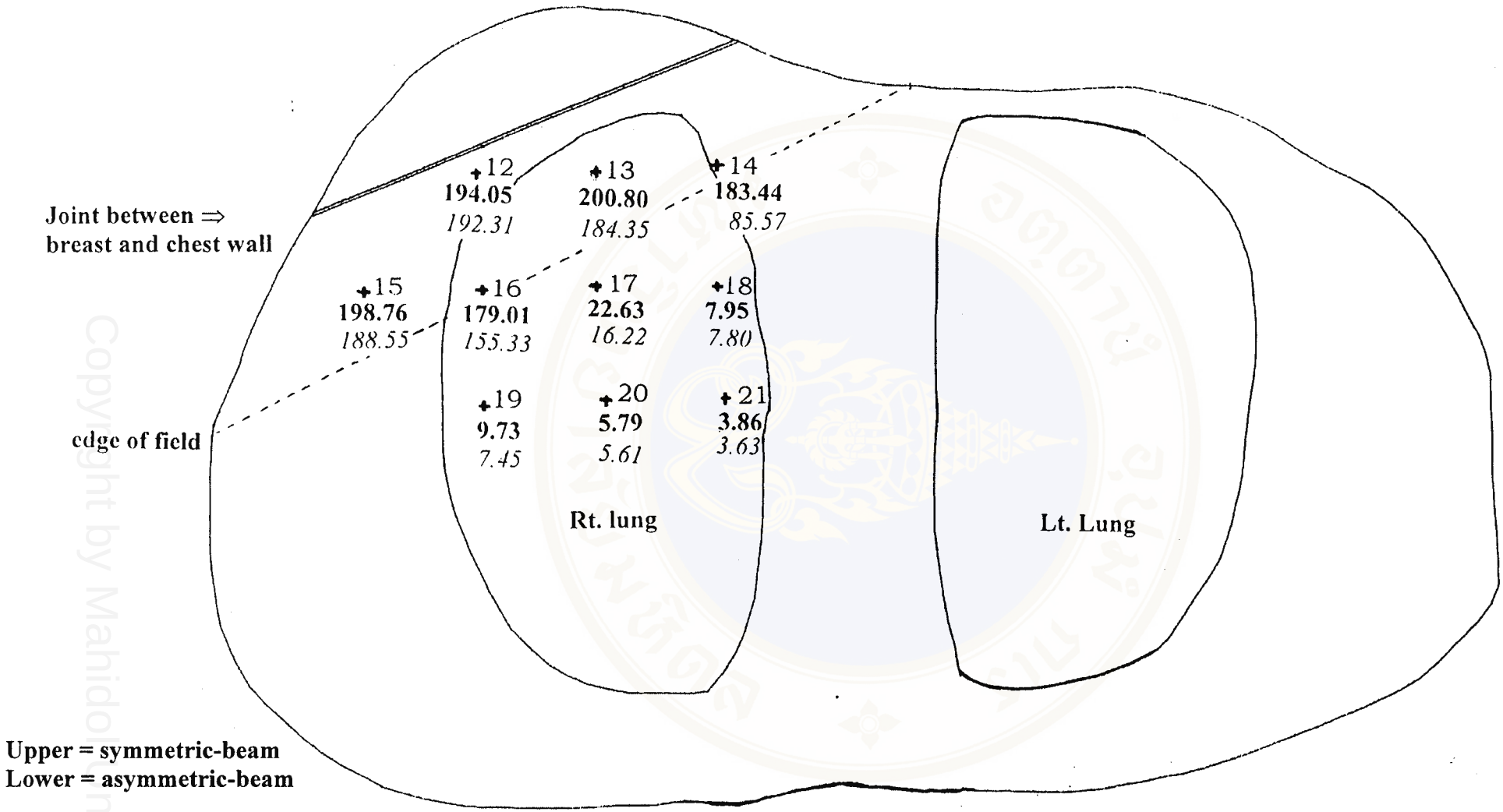

Fig. 26 The absorbed dose measurement at various points in the 15th slab of the rando phantom which is 5 cm upper off axis from the central plane by open beam technique in symmetric and asymmetric beams.

Copyright by Mahidol University

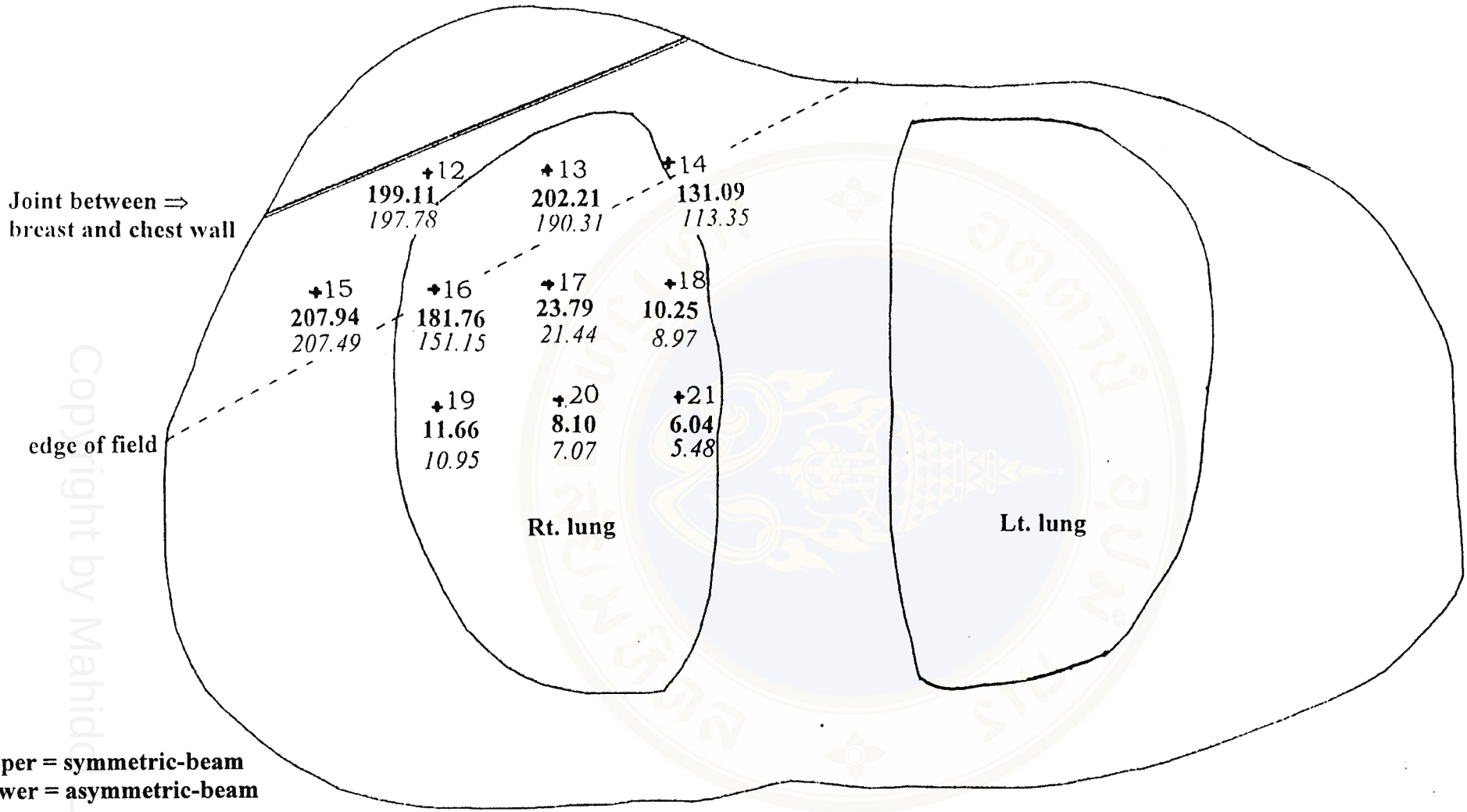

Fig. 27 The absorbed dose measurement at various points in the 15th slab of the rando phantom which is 5 cm upper off axis from the central plane by 15° wedged beam technique in symmetric and asymmetric beams.

Copyright by Mahidol University

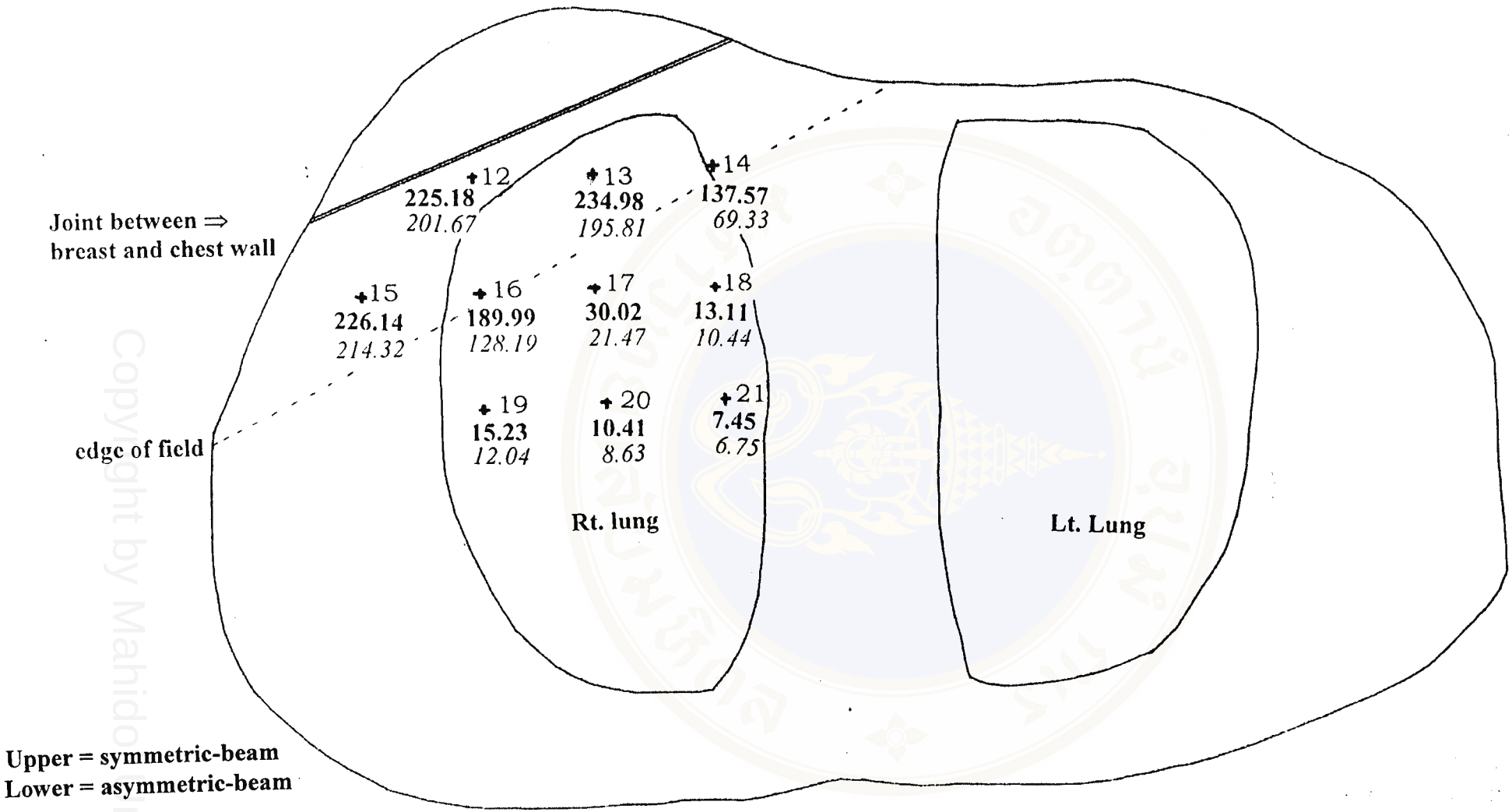

Fig. 28 The absorbed dose measurement at various points in the 15th slab of the rando phantom which is 5 cm upper off axis from the central plane by 30° wedged beam technique in symmetric and asymmetric beams.

Copyright by Mahidol University

Table 8 The absorbed dose measurement at various points in the 19th slab of the chest rando phantom which is 5 cm lower off axis from the central plane in symmetric beams.

Point	Dose measurement (cGy)		
	Open beam	Wedge 15°	Wedge 30°
22	197.98	211.08	210.48
23	177.93	176.32	215.39
24	14.71	16.58	20.90
25	201.89	198.41	204.60
26	47.18	33.06	51.53
27	13.45	13.60	17.05
28	4.83	8.07	9.55
29	6.89	8.46	10.67
30	4.21	6.33	8.34
31	2.98	5.16	6.67

Table 9 The absorbed dose measurement at various points in the 19th slab of the chest rando phantom which is 5 cm lower off axis from the central plane in asymmetric beams.

Point	Dose measurement (cGy)		
	Open beam	Wedge 15°	Wedge 30°
22	171.70	180.67	215.40
23	162.27	162.00	163.42
24	10.91	13.67	14.61
25	163.15	183.74	199.47
26	28.16	22.92	22.09
27	8.47	11.30	12.17
28	5.39	6.58	7.89
29	5.65	7.49	8.83
30	4.25	5.71	7.64
31	4.51	4.47	5.85

Copyright by Mahidol University

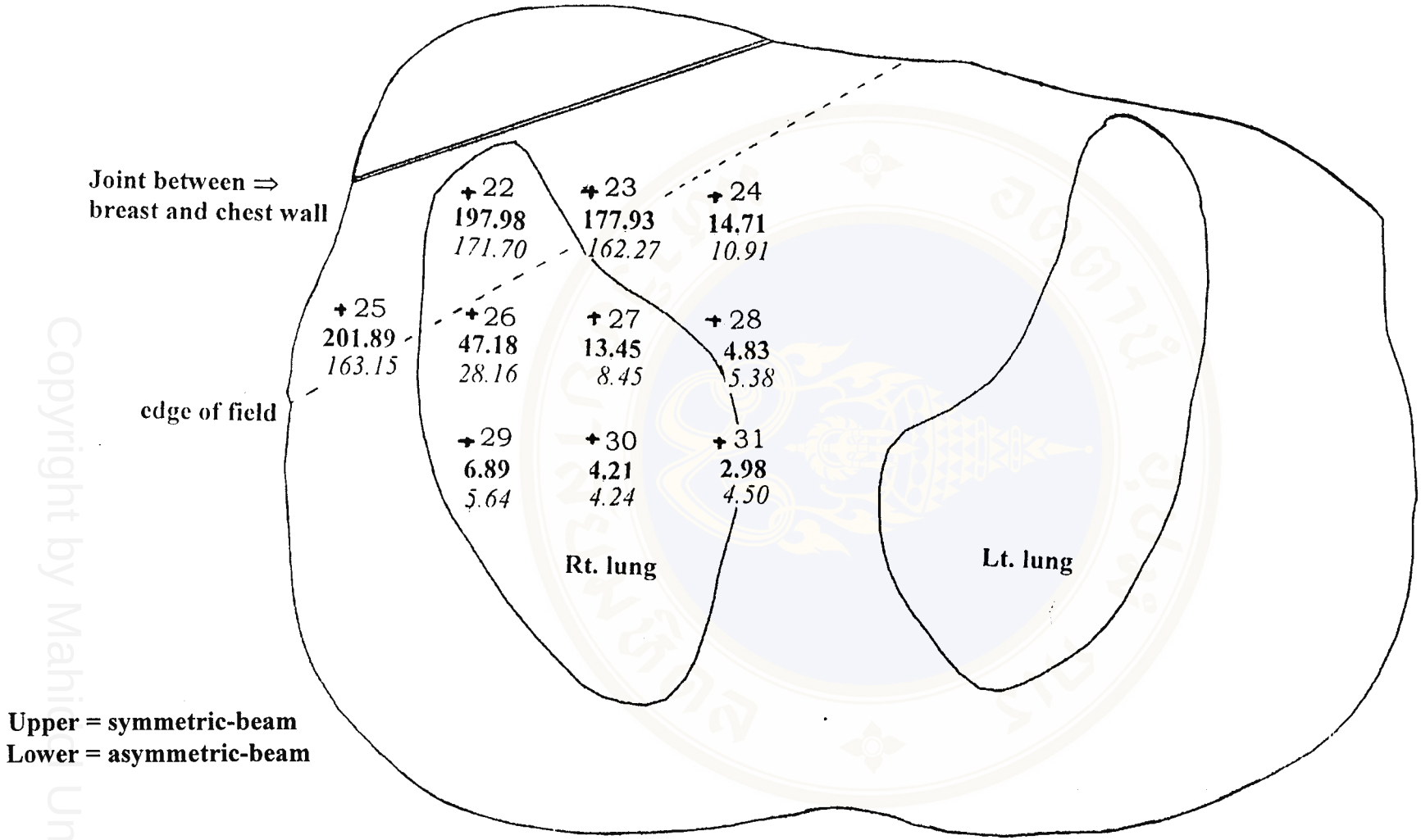

Fig. 29 The absorbed dose measurement at various points in the 19th slab of the rando phantom which is 5 cm lower off axis from the central plane by open beam technique in symmetric and asymmetric beams.

Copyright by Mahidol University

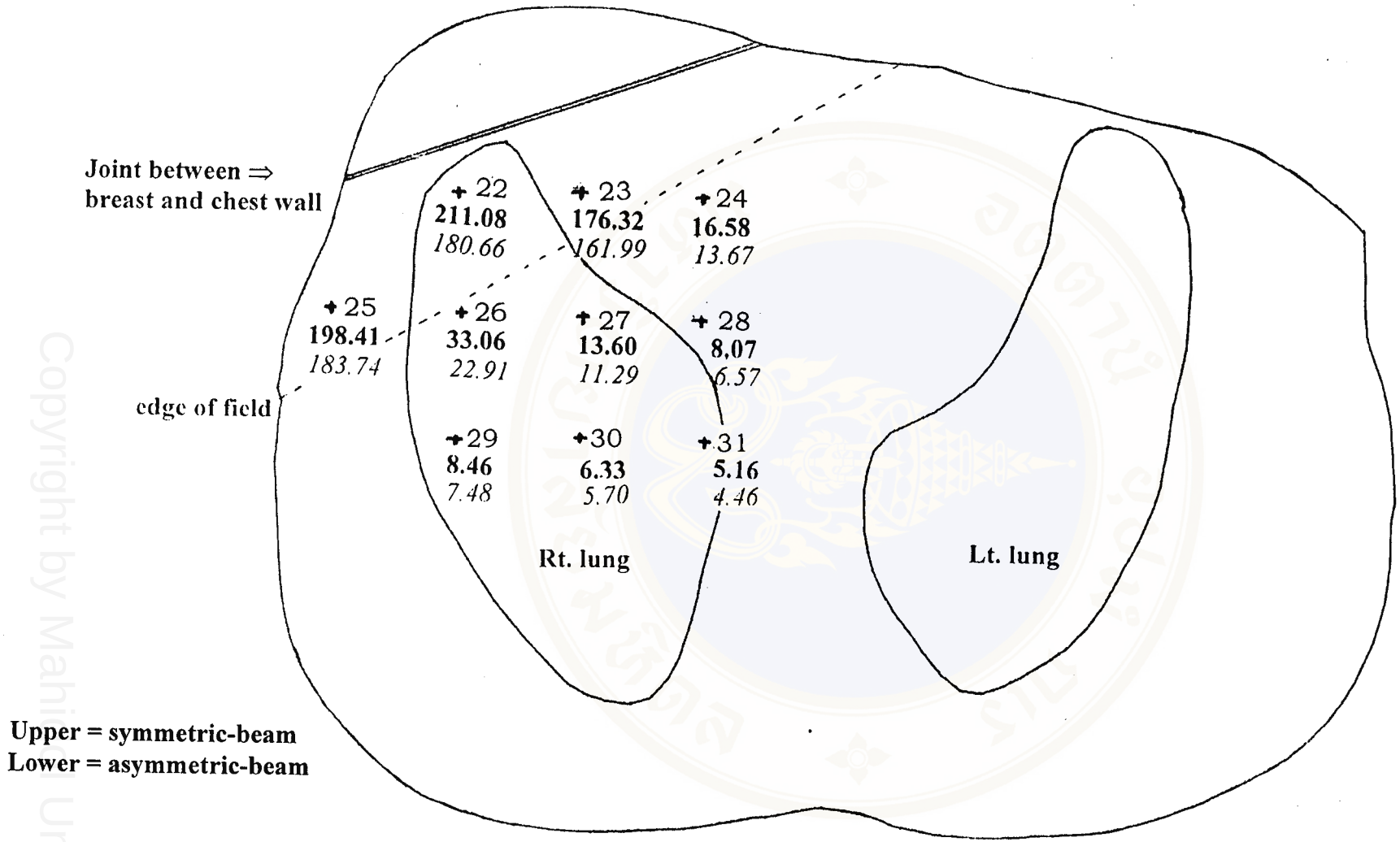

Fig. 30 The absorbed dose measurement at various points in the 19th slab of the rando phantom which is 5 cm lower off axis from the central plane by 15° wedged beam technique in symmetric and asymmetric beams.

Copyright by Mahidol University

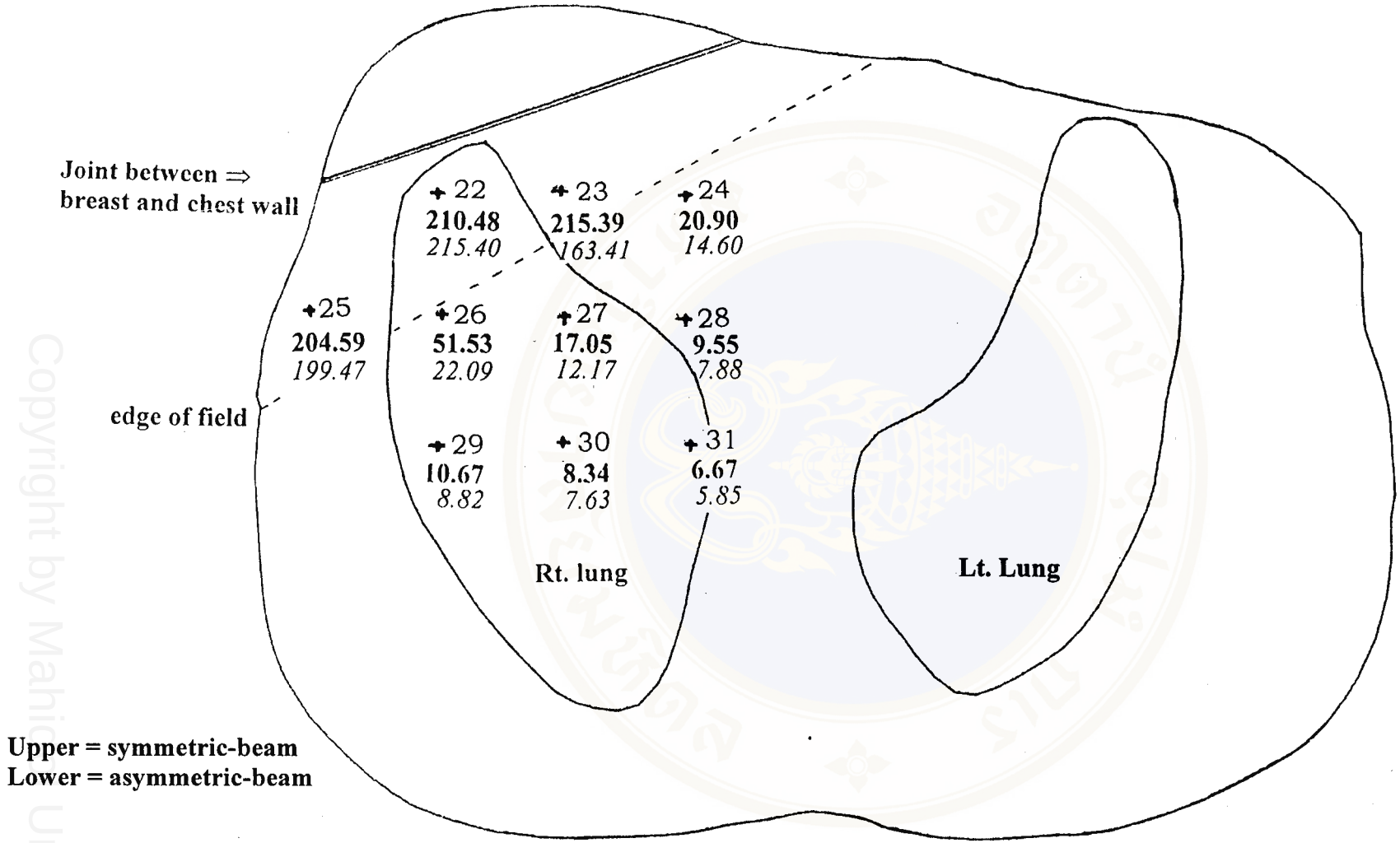

Fig. 31 The absorbed dose measurement at various points in the 19th slab of the rando phantom which is 5 cm lower off axis from the central plane by 30° wedged beam technique in symmetric and asymmetric beams.

Copyright by Mahidol University

Table 10 The comparison of dose distribution in the chest wall from different techniques (the percentage relative dose) at the center, 5 cm upper and 5 cm lower to the central plane, respectively.

Point	The percentage relative dose in the chest wall					
	Sym+open	Sym+W15°	Sym+W30°	Asym+open	Asym+W15°	Asym+W30°
Central plane (in-beam)						
1	89.36	96.26	94.52	86.69	93.02	94.56
5	94.64	95.56	107.75	85.06	90.75	95.08
average	**92.00**	**95.91**	**101.14**	**85.88**	**91.89**	**94.82**
(out-beam)						
4	20.82	18.37	28.97	11.51	13.72	13.86
5cm upper plane (in-beam)						
12	97.03	99.56	112.59	96.16	98.89	113.07
15	99.38	103.97	100.84	94.28	103.75	107.16
average	**98.21**	**101.76**	**106.72**	**95.22**	**101.32**	**110.12**
5cm lower plane (in-beam)						
23	88.97	88.16	107.70	81.14	81.00	81.71
25	100.95	99.21	102.30	81.58	91.87	99.74
average	**94.96**	**93.69**	**105.00**	**81.36**	**86.44**	**90.73**
(out-beam)						
24	7.36	8.29	10.45	5.46	6.84	7.30

Copyright by Mahidol University

Table 11 The comparison of dose distribution in lung tissue from different techniques (the percentage relative dose) at the center, 5 cm upper and 5 cm lower to the central plane, respectively.

Point	The percentage relative dose in lung tissue					
	Sym+open	Sym+W15°	Sym+W30°	Asym+open	Asym+W15°	Asym+W30°
Central plane (in-beam)						
2	92.94	92.09	100.63	85.30	89.57	93.76
3	92.85	95.13	104.32	81.31	85.67	93.63
6	77.06	87.34	92.38	47.65	44.61	50.01
average	**87.62**	**91.52**	**99.11**	**71.42**	**73.28**	**79.13**
(out-beam)						
7	7.78	8.72	10.91	6.49	7.80	7.52
8	3.86	5.09	5.89	3.29	4.35	5.21
9	4.35	5.20	6.56	3.79	4.48	5.25
10	2.62	4.02	5.21	2.32	3.74	4.16
11	1.84	2.97	3.62	1.82	2.77	3.55
average	**4.09**	**5.20**	**6.44**	**3.54**	**4.63**	**5.14**
5cm upper plane (in-beam)						
13	100.40	101.11	117.49	92.18	95.16	97.91
14	91.72	65.55	68.79	42.79	56.68	34.67
16	89.51	90.88	95.00	77.67	75.58	64.10
average	**93.88**	**85.85**	**93.76**	**70.88**	**75.81**	**65.56**
(out-beam)						
17	11.32	11.90	15.01	8.11	10.72	10.74
18	3.98	5.13	6.56	3.90	4.49	5.22
19	4.87	5.83	7.62	3.73	5.48	6.02
20	2.90	4.05	5.21	2.81	3.54	4.32
21	1.93	3.02	3.73	1.82	2.74	3.38
average	**5.00**	**5.99**	**7.63**	**4.07**	**5.39**	**5.94**

Copyright by Mahidol University

Table 11 (continued)

Point	The percentage relative dose in lung tissue					
	Sym+open	Sym+W15°	Sym+W30°	Asym+open	Asym+W15°	Asym+W30°
5cm lower plane (in-beam) 22	98.99	105.54	105.24	85.85	90.33	107.70
(out-beam) 26	23.59	16.53	25.77	14.08	11.46	11.05
27	6.73	6.80	8.53	4.23	5.65	6.09
28	2.42	4.04	4.78	2.69	3.29	3.94
29	3.45	4.23	5.34	2.82	3.74	4.41
30	2.11	3.17	4.17	2.12	2.85	3.82
31	1.49	2.58	3.34	2.25	2.23	2.93
average	**6.63**	**6.23**	**8.66**	**4.70**	**4.87**	**5.37**

Copyright by Mahidol University

3) measurement of surface dose on the rando phantom

(a) target breast

The variation of the percentage relative surface dose on the central plane of rando phantom with different techniques as open beam, 15° and 30° wedged beams in symmetric and asymmetric beams shown in table 12 to 13, respectively. The results show lower percent dose when the wedge angles are increased both symmetric and asymmetric beams. The percentage relative surface dose increase from medial and lateral border to anterior part of the contour, they range from 67.36 to 86.80 , 58.63 to 75.39 and 59.14 to 72.71 of open beam , 15° and 30° wedged beams , respectively for symmetric and 63.75 to 83.10, 60.36 to 78.75 and 59.73 to 73.70 for asymmetric beams.

The comparison of the surface doses between the symmetric and asymmetric beams are shown in Fig. 33 to 35. The surface dose from open symmetric beams seem to be higher than open asymmetric beams but when wedge filters are used, the surface doses from symmetric beams are comparable to asymmetric beams. The graph could not be distinguished between symmetric and asymmetric beams. The data in table 12 and 13 are plotted in Fig. 35 . The graph shows that the percentage relative surface doses are the highest when the open symmetric beams are used and they are relative low when 30° wedge symmetric and asymmetric beams are used.

Copyright by Mahidol University

293627 i 11782018

Table 12 The variation of the percentage relative surface dose on the rando phantom with different wedge angles in symmetric beams techniques.

Position of TLD	The percentage relative surface dose		
	Open-beam	Wedge 15°	Wedge 30°
#1	70.19	65.48	59.14
#2	83.59	75.39	72.71
#3	86.80	69.58	69.87
#4	72.99	66.41	61.23
#5	67.36	58.63	61.73

Table 13 The variation of the percentage relative surface dose on the rando phantom with different wedge angles in asymmetric beams techniques.

Position of TLD	The percentage relative surface dose		
	Open-beam	Wedge 15°	Wedge 30°
#1	67.79	70.71	67.23
#2	83.10	70.85	67.13
#3	79.88	78.75	73.70
#4	70.46	64.84	62.40
#5	63.75	60.36	59.73

Copyright by Mahidol University

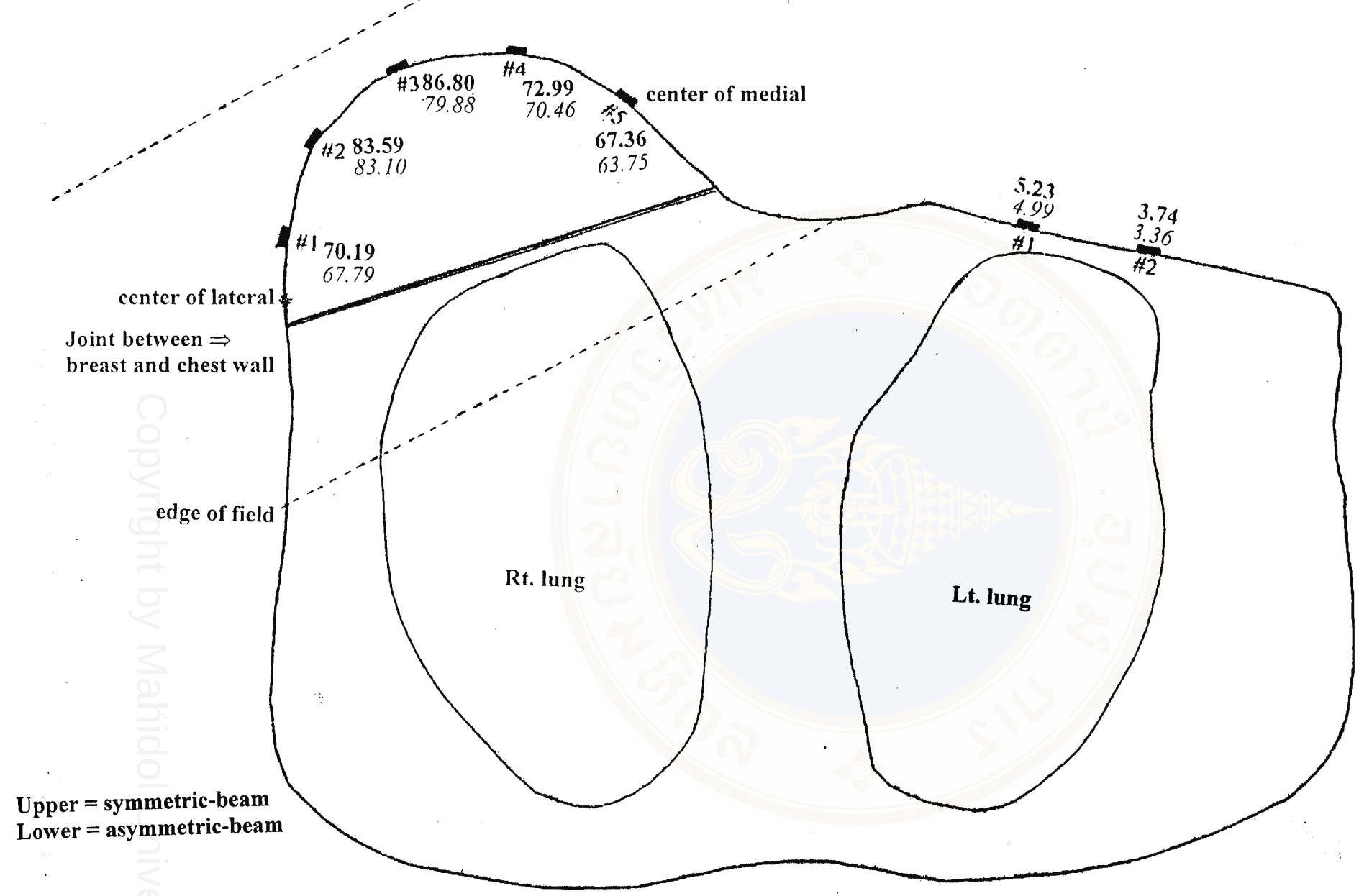

Fig. 32 The percentage relative surface dose which is in the central plane by open beam technique in symmetric and asymmetric beams.

Copyright by Mahidol University

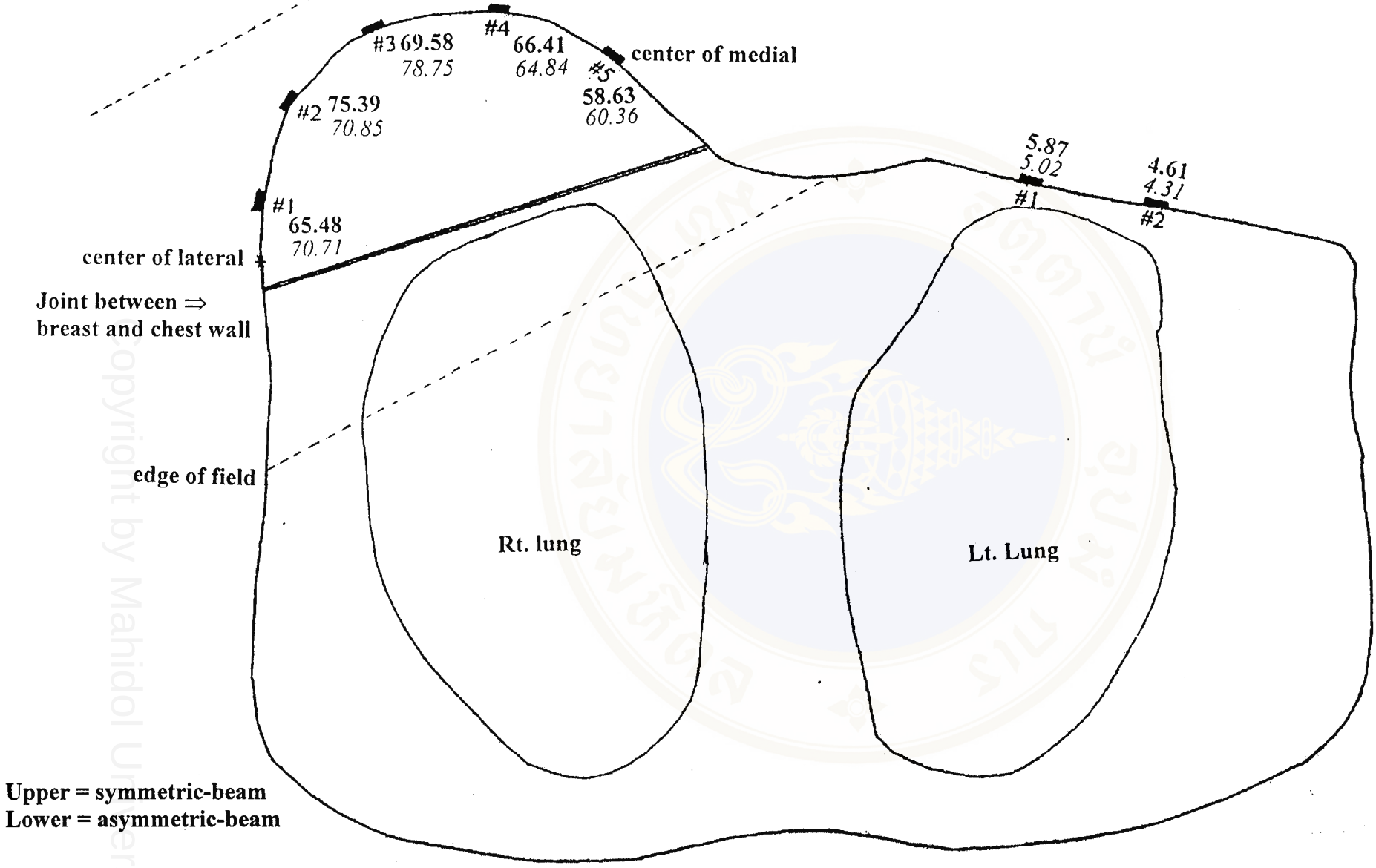

Fig. 33 The percentage relative surface dose which is in the central plane by 15° wedged beam technique in symmetric and asymmetric beams.

Copyright by Mahidol University

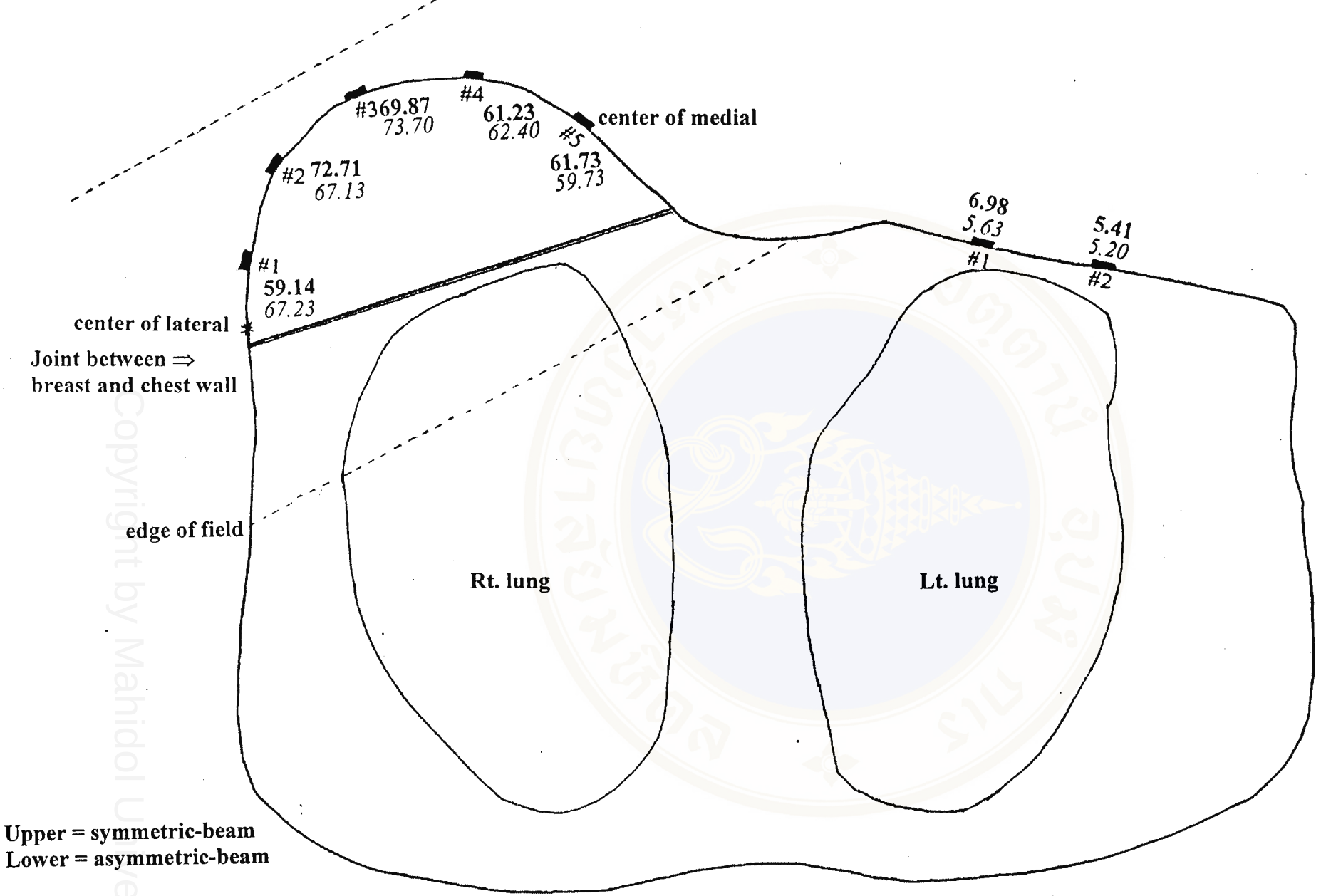

Fig. 34 The percentage relative surface dose which is in the central plane by 30° wedged beam technique in symmetric and asymmetric beams.

Copyright by Mahidol University

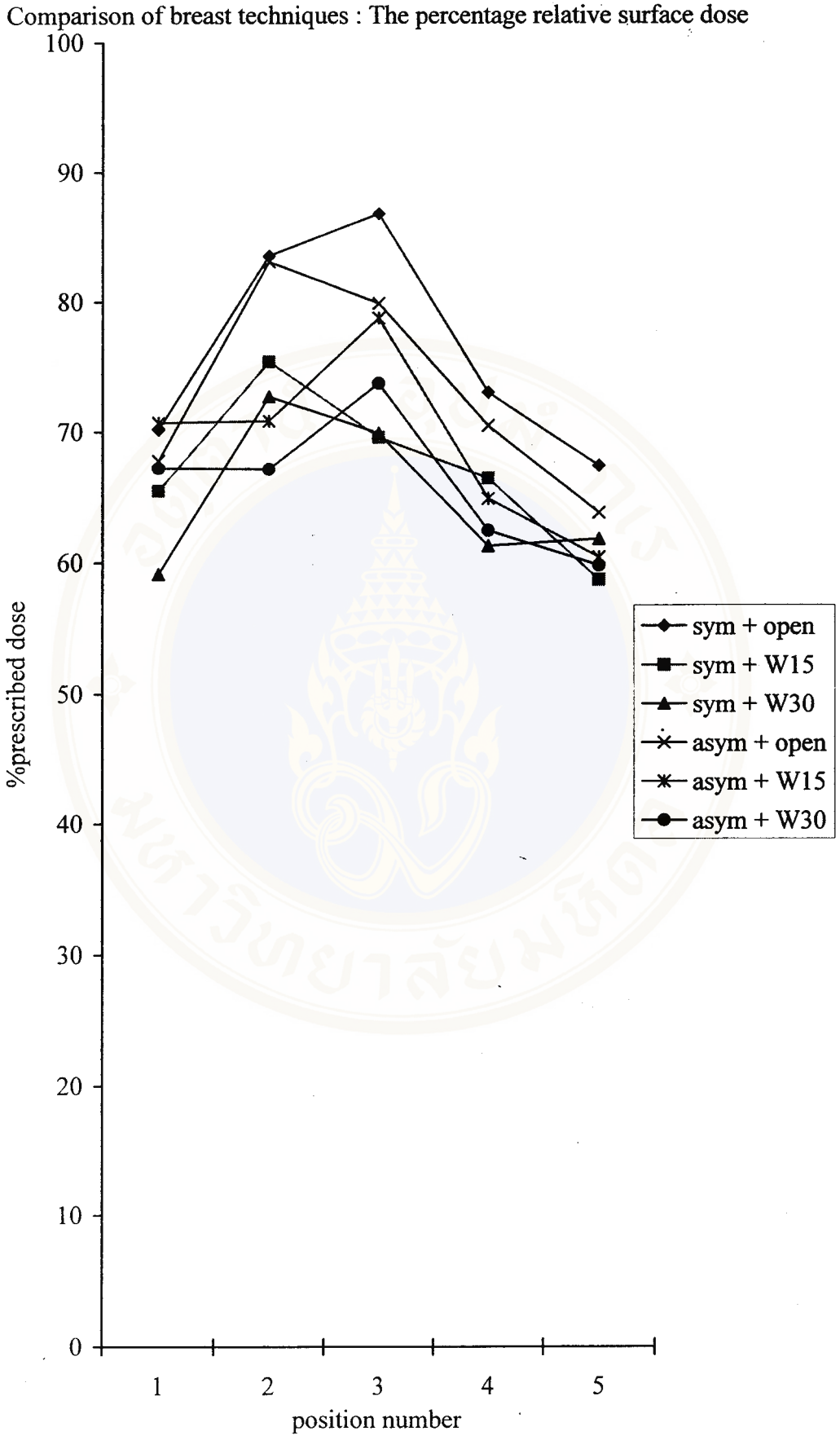

Fig. 35 Comparison of the percentage relative surface dose to the breast phantom of symmetric and asymmetric beams with and without wedges.

Copyright© by Mahidol University

(b) contralateral breast

The variation of the percentage surface doses relative surface dose on the rando phantom with different wedge angle in symmetric and asymmetric beams techniques at the contralateral breast are shown in table 14 and 15, respectively. The percentage relative surface doses are shown in Fig 32 to 34 as a function of TLD capsule position. The percentage relative surface dose at contralateral breast range from 3.74 to 5.23, 4.61 to 5.87 and 5.41 to 6.98 of open beam , 15° and 30° wedged beams , respectively for symmetric beams and 3.36 to 4.99, 4.31 to 5.02 and 5.20 to 5.65 for asymmetric beams. Fig. 36 show a graph comparing of the percentage relative surface dose at point #1 which is about at 5 cm laterally from the edge of the medial tangential field.

The contralateral dose show higher dose when the larger degree of wedge are used, the effect is more with the symmetric beams. The wedge filter gives less effect in asymmetric beams.

Copyright by Mahidol University

Table 14 The variation of the percentage relative surface dose on the rando phantom with different wedge angles in symmetric beams techniques at the contralateral breast.

Position of TLD	The percentage relative surface dose		
	Open-beam	Wedge 15°	Wedge 30°
#1	5.23	5.87	6.98
#2	3.74	4.61	5.41

Table 15 The variation of the percentage relative surface dose on the rando phantom with different wedge angles in asymmetric beams techniques at the contralateral breast.

Position of TLD	The percentage relative surface dose		
	Open-beam	Wedge 15°	Wedge 30°
#1	4.99	5.02	5.65
#2	3.36	4.31	5.20

Copyright by Mahidol University

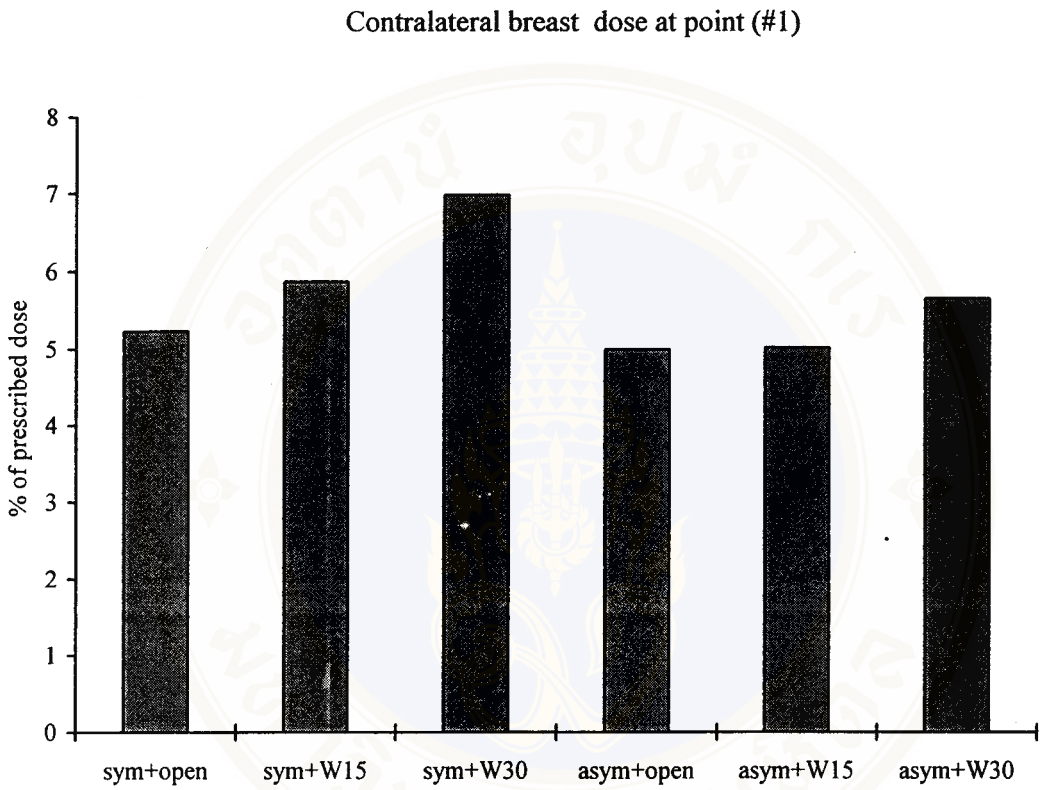

Fig. 36 Comparison of the percentage relative surface dose at point #1 of the contralateral breast in different techniques.

Copyright by Mahidol University

5.1.3 Measurement of surface dose on the patients.

(a) Target breast

The variation of the percentage relative surface dose on the patients with different techniques as open beam, 15° and 30° wedged beams in symmetric and asymmetric beams are shown in table 16 and 17 , respectively. The percentage relative surface doses increase from medial and lateral border to anterior part of the contour, they range from 60.50 to 88.03, 59.96 to 82.43 and 59.72 to 81.67 for symmetric beams of open beam, 15° and 30° wedged beams, respectively. Asymmetric beams contribute higher dose in the patients than the phantom, the percentage values range from 70.45 to 100.49, 62.15 to 85.59 and 60.16 to 80.24 for asymmetric beams. In Fig. 37, the graphs show that open asymmetric beam gives the highest dose at position 3.

Copyright by Mahidol University

Table 16 The variation of the percentage relative surface dose on the patients with different wedge angles in symmetric beams techniques.

Position of TLD	The percentage relative surface dose		
	Open-beam	Wedge 15°	Wedge 30°
#1	60.50	59.96	59.72
#2	66.92	71.04	70.17
#3	79.55	78.47	77.77
#4	88.03	82.43	81.67
#5	76.99	70.85	70.15

Table 17 The variation of the percentage relative surface dose on the patients with different wedge angles in asymmetric beams techniques.

Position of TLD	The percentage relative surface dose		
	Open-beam	Wedge 15°	Wedge 30°
#1	71.73	65.27	60.16
#2	81.94	71.29	69.54
#3	100.49	85.59	80.24
#4	81.41	76.16	74.60
#5	70.45	62.15	62.01

Copyright by Mahidol University

Comparison of breast techniques : The percentage relative surface dose

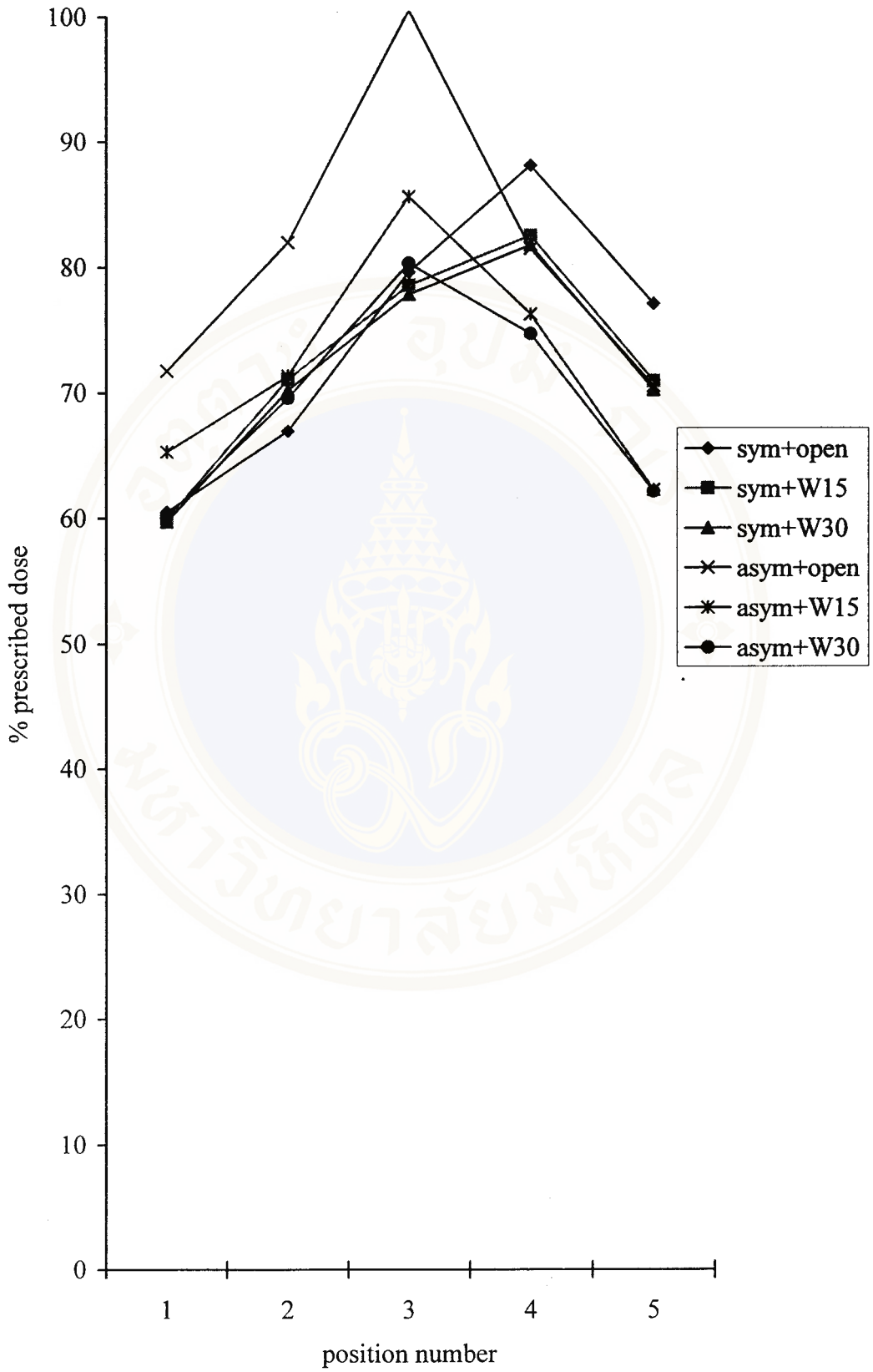

Fig. 37 Comparison of the percentage relative surface dose to the breast on the patients in symmetric and asymmetric beams with and without wedges.

(b) contralateral breast

The variation of the percentage relative surface doses on the patients with different techniques as open beam, 15° and 30° wedged beams in symmetric and asymmetric beams are shown in table 18 and 19, respectively. The percentage relative surface doses at contralateral breast range from 0.82 to 1.89, 1.48 to 2.14 and 1.74 to 2.38 of open beam , 15° and 30° wedged beams, respectively for symmetric beams and 2.10 to 3.96, 2.63 to 4.39 and 2.92 to 4.57 for asymmetric beams. Fig. 38 shows a graph comparing of the percentage relative surface dose at point #1 which is about at 5 cm lateral from the edge of the medial tangential field.

The contralateral doses show higher dose when the larger degree of wedge are used, the effect is more with the asymmetric beams.

Copyright by Mahidol University

Table 18 The variation of the percentage relative surface dose on the patients with different wedge angles in symmetric beams techniques at the contralateral breast.

Position of TLD	The percentage relative surface dose		
	Open-beam	Wedge 15°	Wedge 30°
#1	1.89	2.14	2.78
#2	0.82	1.48	1.74

Table 19 The variation of the percentage relative surface dose on the patients with different wedge angles in asymmetric beams techniques at the contralateral breast.

Position of TLD	The percentage relative surface dose		
	Open-beam	Wedge 15°	Wedge 30°
#1	3.96	4.39	4.57
#2	2.10	2.63	2.92

Copyright by Mahidol University

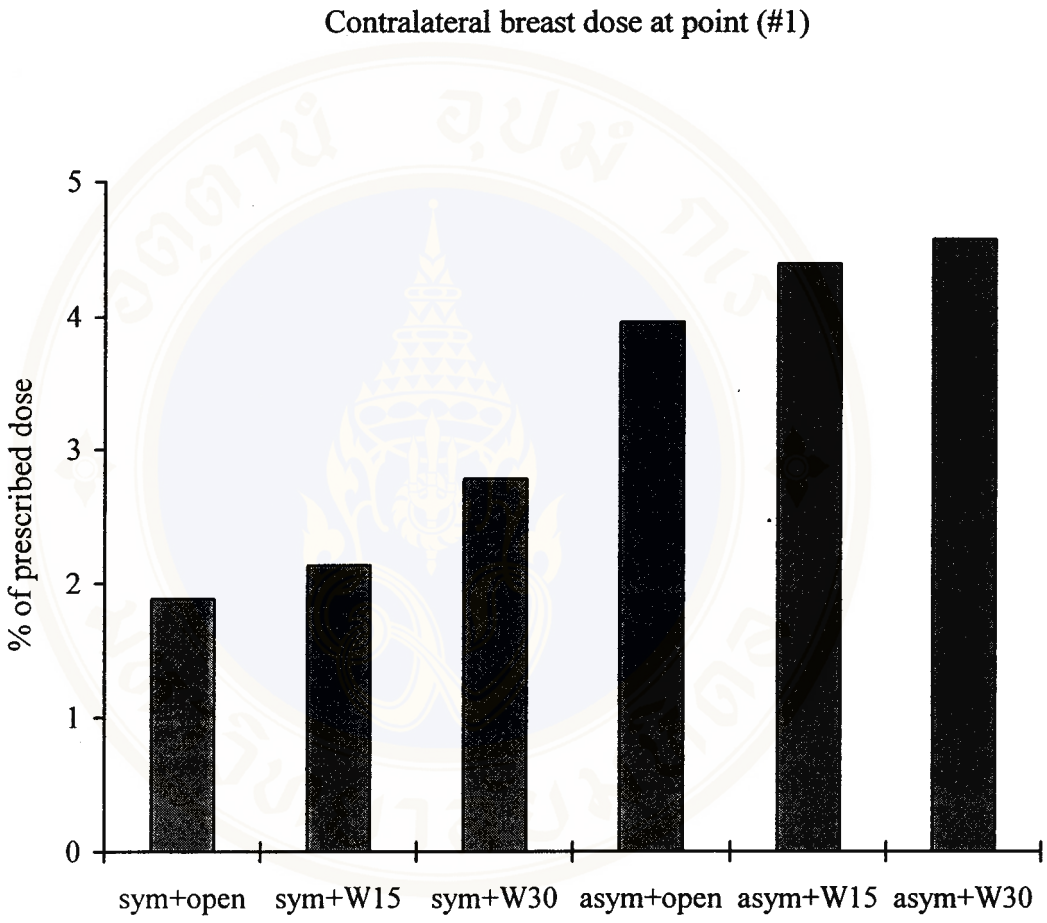

Fig. 38 Comparison of the percentage relative surface dose at point #1 of the contralateral breast on the patients in different techniques.

Copyright by Mahidol University

CHAPTER VI

DISCUSSION AND CONCLUSION

The purpose of this study was to evaluate the influence of various techniques commonly used in breast cancer treatment on doses received in points of interest inside and outside the treatment volume. This investigation has shown that:

1. The absorbed doses measured at reference points (average dose at point A_4 and A_5) in coronal plane of breast phantom are very close to the prescribed dose of 200 cGy from the comparison of six irradiation techniques. The maximum different are 4.03% for open symmetric beam. The upper transverse plane of all techniques show higher dose than the central plane, the maximum of the percentage relative dose is 111.86 for 30° wedge symmetric beam. The lower transverse plane of all techniques show lower dose than the central transverse plane, the minimum of the percentage relative dose is 84.64 for open asymmetric beam. These effect are caused by the anatomical of the breast contour in which the lower contour is wider than the upper contour.

The asymmetric beams give less inhomogeneity compare to symmetric beams. The divergence of asymmetric beams together with the shape of contour may influence the homogeneity effect.

Wedge filter are not ideal compensators for breast (22), since they do not compensate the curvature of the breast in the longitudinal direction of the patient.

Copyright by Mahidol University

This study confirms inhomogeneity dose in coronal plane even the wedge filters are used.

2. The doses at chest wall and lung inside and outside the treatment area of symmetric and asymmetric beams are increased with the larger degree of wedge angle. When chest wall and lung doses inside and outside the treatment fields for six techniques and all three planes are averaged, the percentage relative chest wall doses are 95.96 and 12.75, respectively. The average percentage relative lung doses inside and outside the treatment field are 87.86 and 5.53, respectively.

The chest wall and lung doses are decreased significantly when using asymmetric beam, but the other factors also influence which include the degree of wedge filter used, the angle of the incidence beams and the anatomical of the patient.

3. The surface doses on the target breast phantom in the central transverse plane are decreased significantly when the larger degree of wedge angle are used. The doses of open symmetric beam is slightly higher than the open asymmetric beam, but the wedge filter give the comparable dose.

The surface dose is higher at the apex than medial and lateral beams of the breast. The highest value of percentage relative dose in six techniques range from 67.33 to 86.80 when the open symmetric beam is used. The technique which contributes the lowest surface doses is 30°wedge symmetric beam with the percentage relative dose range from 59.14 to 72.71.

Contrary to the target breast, surface doses at contralateral breast are higher when the larger degree of wedge angles are used and the asymmetric beams contribute less scatter dose. The lowest percentage relative contralateral surface dose in open asymmetric beam gives 4.99 at 5 cm from the edge of the beam.

Copyright by Mahidol University

4. The surface doses to the skin of the patients undergoing x-ray radiotherapy depend on a number of parameters such as electron contamination of the original beam, field size, beam accessory devices, patient geometry and obliquity of the beam (23).

The surface doses in the target and contralateral breast in the patients are different from the phantom. However, when the larger degree of wedge filters are used, the surface doses of both patient and phantom are decreased while the contralateral surface doses of both are increased.

The contralateral surface doses of the patients using asymmetric beams are higher than symmetric beams which contrast to the measurement in the phantom.

The course of discrepancy of doses in the patients and the phantom are the variation of breast size and shape which differ from the phantom. In addition, the measurement in the patients were performed in one sample for each technique, therefore the conclusion can not be drawn.

Tercilla et. al. presented data of contralateral breast dose on the patients treated with half-beam block SSD-technique in Co-60 beams. The percentage relative contralateral breast dose range from 6.45 to 12.89 (24).

In this study a distance of 5 cm lateral from the edge of the medial tangential field was chosen because this point usually falls half way between the patient's midline and the apex of the contralateral breast. It is well outside the beam penumbra, and a significant amount of contralateral breast tissue is present at this distance (25). However, the phantom is rigid and the breast does not fall laterally as a natural breast might be. Thus, the phantom does not represent the real breast that we see in our patients. The effect of this rigidity in the phantom is that the contralateral breast

Copyright by Mahidol University

remains closer to the edge of the beam, which may give higher doses in the phantom than would be found in the real patients contralateral breast.

We can conclude that the information gained from the measurement in the phantom can be induced the understand of how the absorbed doses vary inside and outside the treatment field in different techniques. The over and underdoses can be prevented by choosing the appropriated technique for each patient.

Copyright by Mahidol University

REFERENCES

1. The Faculty of Medicine Ramathibodi Hospital Mahidol University. Ramathibodi Cancer Registry, 1997 Annual Report.
2. Kelly CA, Wang XY, Chu JCH, Hartsell WF. Dose to contralateral breast : A comparison of four primary breast irradiation techniques. Int. J. Radiation Oncology. Biol. Phys 1996 ; 34 (3) : 727-32.
3. Williams JR, Thwaites DI. Asymmetric collimators. In : Radiotherapy physics in practice. New York, 1993 : 142,172.
4. Rosenow UF, Valentine ES, Davis LW. A technique for treating local breast cancer using a single set-up point and asymmetric collimator. Int. J. Radiation Oncology. Biol. Phys 1990 ; 19 : 183-8.
5. Bentel GC, Nelson CE, Thomas KN. Treatment planning breast. In : Treatment planning and dose calculation in radiation oncology. 4th ed. New York : Mcgraw-Hill, 1993 : 226-41.
6. Bentel GC, Nelson CE, Thomas KN. Treatment planning in radiation oncology. In : Treatment planning and dose calculation in radiation. 3rd ed. New York: Pergamon, 1982 : 192.
7. Orton CG, Seibert JB. Depth dose in skin for obliquely incident Co^{60} radiation. The British. J. of Radiology 1972 ; 45 : 271.
8. James CD. Irradiation technique for the breast or chest wall. In : Moss' Radiation oncology rationale, technique, results. 7th ed. St. Louis, Missouri : Mosby-year book, 1994 : 383-9.

Copyright by Mahidol University

9. Podgorsak EB, Gosselin M, Kim TH, Freeman CR. A simple isocentric technique for irradiation of the breast, chest wall and peripheral lymphatics. The British J. of Radiology 1984 ; 57 (673) : 57-63.

10. Kwa W, Xornelsen RO, Harrison RW, Khatib EE. Dosimetry for asymmetric x-ray fields. Med Phys 1994 ; 21 (10) : 1599-1604.

11. William K, Victor T, Randall FN, Stewart JM, Ellen KE, Robert HW. Clinical use of asymmetric collimation. Int. J. Radiation Oncology. Biol. Phys 1997 ; 37 (30) : 705-10.

12. Khan FM, Gerbi BJ, Deibel FC. Dosimetry of asymmetric x-ray collimations. Med Phys 1986 ; 13 (6) : 936-41.

13. Palta JR, Ayyangar KM. Dosimetric characteristic of 6 Mvphoton beam from a linear accelerator with asymmetric collimator jaws. Int. J. Radiation Oncology. Biol. Phys 1998 ; 14 : 383-7.

14. Khan FM. Measurement of absorbed dose. In : The Physics of radiation therapy. 2nd ed. Baltimore :Williams & Wilkins, 1994 :167-71,179-81,214-5,236,286.

15. Khan FM. dosimetry of wedge fields with asymmetric collimation. Med. Phys 1993 ; 20 (5) : 1447-51.

16. Niroomand-Rad A, Haleem M, Rodgers JE, Obcemea C. Wedge factor dependence on depth and field size for various beam energies using symmetric and half-collimated asymmetric jaw setting. Med. Phys 1992 ; 19 (6) : 1445-50.

17. Niroomand-Rad A, Rodgers JE, Taylor P, Hames B. Dosimetric parameters of a modified set of wedges for use with asymmetric fields of a 6 MV linear accelerator. Med. Phys 1994 ; 21 (9) : 1405-8.

Copyright© by Mahidol University

18. John HE, Cunningham JR. Thermoluminescent dosimetry (TLD) In : The physics of radiotherapy. 4th ed. Illinois : Charles C Thormus, 1983 : 317-9.

19. Mckinlay AF. The characteristics of thermoluminescence material. In : Medical physics Hand Books Thermoluminescence Dosimetry: Bristol : Adam Hilger, 1981 : 32-3, 83,132-3.

20. Instruction Manual for PTW-TLD oven valid for S/N 1400 or greater.

21. Harshaw bicon radiation measurement produced. Model 5500 automatic TLD reader user's Manual Ohio : Saint-Gobain / Norton industrial ceramics, 1993 : 1.

22. Chin LK, Cherg CN, Siddon RL, Rice RK, Miznheer BJ, Harris JR. Three dimensional photon dose distribution with and without lung correction for tangential breast intact treatments. Int. J. Radiation Oncology. Biol. Phys 1989 ; 17 : 1327-35.

23. Kron T, Elliot A, Wong T, Showell G, Clubb B, Metcalfe P.X-Ray surface dose measurements using TLD extrapolation. Med. Phys 1993 ; 20 (3) : 703-11.

24. Tercilla O, Krasin F, Lawn-Tsao L. Comparison of contralateral breast dose from 1/2 beam block and isocentric treatment techniques for patient treated with primary breast irradiation with ^{60}Co. Int. J. Radiation Oncology. Biol. Phys 1989 ; 17 : 205-10.

25. Runkel RM, Kalokhe UP. Scatter dose from tangential breast irradiation to the uninvolved breast. Radiology 1990 ; 175 : 873-6.

293627

Copyright by Mahidol University

BIOGRAPHY

NAME Miss. Pachuen Potup

DATE OF BIRTH 25 January 1974

PLACE OF BIRTH Uttaradit, Thailand

INSTITUTIONS ATTENDED

Mahidol University , 1992-1996 :
Bachelor of Science (Radiological Technology)
Mahidol University , 1996-1998 :
Master of Science (Medical Physics)

RESEARCH GRANT Research Grant from Faculty of Graduate Studies, Mahidol University in the academic year of 1997

Copyright by Mahidol University